ARPHA Preprints

PENSOFT

PREPRINT

Author-formatted, not peer-reviewed document posted on 24/11/2021

DOI: https://doi.org/10.3897/arphapreprints.e78423

Potential distribution of invasive boxwood blight pathogen (*Calonectria pseudonaviculata*) as predicted by process-based and correlative models

Brittany Barker, Leonard Coop, Chuanxue Hong

Potential distribution of invasive boxwood blight pathogen (*Calonectria pseudonaviculata*) as predicted by process-based and correlative models

Brittany S. Barker[1,2*], Leonard Coop[1,2], Chuanxue Hong[3]

[1]Oregon Integrated Pest Management Center, 4575 Research Way, Oregon State University, Corvallis, OR 97331 USA

[2]Department of Horticulture, Oregon State University, 4017 Agriculture and Life Sciences Building, Oregon State University, Corvallis, OR 97331 USA

[3]Hampton Roads Agricultural Research and Extension Center, Virginia Polytechnic Institute and State University, 1444 Diamond Springs Road, Virginia Beach, VA 23455 USA

*Corresponding author: Brittany Barker
E-mail: brittany.barker@oregonstate.edu

Key words: *Buxus*; plant disease; invasion; climatic suitability; CLIMEX; ensemble

Open Research Statement: The data, metadata, code, and derived products to reproduce the analysis and figures are currently available for reviewer access at GitHub repository (https://github.com/bbarker505/Cps-climSuit-modeling). Please note that site information for seven records from Oregon used for modeling are not provided due to confidentiality concerns. The final version of this repository will be archived at Zenodo.org or protocols.io prior to publication of this manuscript.

Abstract

Boxwood blight, caused by the ascomycete fungi *Calonectria pseudonaviculata* and *C. henricotiae*, is an emerging plant disease of boxwood (*Buxus* spp.) that has had devastating impacts on the health and productivity of boxwood in both the horticultural sector and native ecosystems. In this study, we predicted the potential distribution of *C. pseudonaviculata* at regional and global scales and explored how climatic factors shape its known range limits. Our workflow combined multiple modeling algorithms to enhance the reliability and robustness of predictions. We produced a process-based climatic suitability model in the CLIMEX program and combined outputs of six different correlative modeling algorithms to generate an ensemble correlative model. All models were fit and validated using an occurrence record dataset (N = 292 records from 24 countries) comprised of positive detections of *C. pseudonaviculata* from across its entire known invaded range. Evaluations of model performance provided validation of good model fit for all models. A consensus map of CLIMEX and ensemble correlative model predictions indicated that not-yet-invaded areas in eastern and southern Europe and in the southeastern, midwestern, and Pacific coast regions of North America are climatically suitable for establishment. Most regions of the world where *Buxus* and its congeners are native are also at risk of establishment, which suggests that *C. pseudonaviculata* should be able to significantly expand its range globally if susceptible hosts exist. Our findings provide the first insight into the global invasion threat of boxwood blight, and are valuable to stakeholders who need to know where to focus surveillance efforts for early detection and rapid response measures to prevent or slow the spread of the disease.

Introduction

Invasive plant pathogens are a global threat to the health, productivity, and diversity of plants in both agricultural and native ecosystems (Fisher et al. 2012, Lovett et al. 2016, Paini et al. 2016, Thakur et al. 2019). Plant pathogens including viruses, bacteria, oomycetes and fungi have been dispersing at unprecedented levels owing to increasing global trade and human travel, often remaining undetected or unidentified until they have spread and created visible impacts on hosts and recipient ecosystems (Fisher et al. 2012, Ricciardi et al. 2017, Thakur et al. 2019). In forest ecosystems, anthropogenic introductions of fungal and fungal-like pathogens are the main cause of emerging infectious diseases in trees, such as the well-known examples of chestnut blight and Dutch elm disease in North America (Lovett et al. 2016, Thakur et al. 2019). Ascomycete plant pathogens that can infect multiple host species in cultivated (e.g., parks, gardens, orchards, or nurseries) and native ecosystems tend to be particularly invasive, and include some of the most destructive pests of forest trees in countries with high levels of live plant trade (Santini et al. 2013, Lovett et al. 2016, Nahrung and Carnegie 2020).

Boxwood blight, also known as box blight, is an emerging disease of species in the genus *Buxus*, many of which are major evergreen shrub crops and iconic landscape plants (Batdorf 2005, Daughtrey 2019, Hong 2019b), as well as a keystone forest species (Kolganikhina 2014, Matsiakh 2016, Mitchell et al. 2018, Şimşek et al. 2019). This disease is caused by two invasive ascomycete fungi, *Calonectria pseudonaviculata* (*Cps*) (Lombard et al. 2010) and *C. henricotiae* (Gehesquière et al. 2016). Both pathogen species can infect and blight boxwood foliage, resulting in rapid plant death. *Calonectria henricotiae* is only known to occur in Europe, whereas *Cps* has a wider distribution that presently spans 24 countries primarily in Europe, Asia, and North America (Gehesquière et al. 2016, Daughtrey 2019, Castroagudín et al. 2020a, EPPO 2020). *Cps* typically disperses long distances through human-mediated transport of diseased liners (young plants) and nursery stock (Gehesquière 2014, Daughtrey 2019), often going undetected because plants can be asymptomatic until exposed to weather patterns favoring infection and subsequent symptom development (Gehesquière et al. 2013, LeBlanc et al. 2018). After the initial detection of *Cps* in the United Kingdom in 1994 (Henricot et al. 2000), the pathogen was reported from New Zealand in 1998 (Crous et al. 2002) and had spread to at least eight countries in continental Europe by 2013 (Palmer and Shishkoff 2014). *Cps* was first

detected in western Asia in 2010, and has since become widespread throughout native *Buxus* forests in the Black Sea region of Turkey and the Caucasus (Gorgiladze et al. 2011, Akili et al. 2012, Gasich et al. 2013) up to the Caspian Hyrcanian forests of northern Iran (Mirabolfathy 2013, Rezaee et al. 2013, Khazaeli et al. 2018). Initial reports of *Cps* in North America in 2011 and 2012 were from the east coast of the United States (Douglas 2012, Ivors et al. 2012) and in Oregon (Anonymous 2012) and British Columbia (Elmhirst et al. 2013), but the pathogen has now been documented in at least 30 U.S. states throughout the Southeast, Northeast, Midwest, and Pacific coast (Castroagudín et al. 2020b, Hall et al. 2021).

Boxwood blight caused by *Cps* poses a serious threat to the horticultural industry, local economies, and ecosystem integrity (LeBlanc et al. 2018, Mitchell et al. 2018, Daughtrey 2019). In the United States, the ornamental horticulture industry has sustained significant financial losses because boxwood is the number one evergreen shrub sold, with an annual wholesale value greater than $140 million (USDA National Agricultural Statistics Service 2020). Boxwood blight increases the cost of producing boxwood because infected plants are unsellable and must be destroyed, and controlling the disease with chemical treatments is expensive (LaMondia 2015, Daughtrey 2019, Hall et al. 2021). Total economic losses resulting from boxwood blight in Connecticut alone amounted to more than $3 million within the first year of detection (LaMondia 2015). Additionally, the disease has caused declines in native *Buxus* forests in western Asia, which has reduced habitat for *Buxus*-associated biodiversity and negatively impacted ecosystem services (Mirabolfathy et al. 2013, Matsiakh 2016, Lehtijärvi et al. 2017, Mitchell et al. 2018). The full host range of *Cps* is unknown; however, none of 11 tested *Buxus* species were immune to boxwood blight (Henricot et al. 2008, Shishkoff et al. 2015, LaMondia and Shishkoff 2017), and certain Buxaceae plants in the genera *Sarcococca* Lindl. (Henricot et al. 2008, Malapi-Wight et al. 2016, Ryan et al. 2018) and *Pachysandra* Michx. (LaMondia et al. 2012, LaMondia and Li 2013, Kong et al. 2017) are also vulnerable to infection. Artificial inoculations demonstrated that the host range may even include plants in other taxonomic families (Richardson et al. 2020). These findings suggest that *Cps* could be a significant threat to at least some of the *ca.* 100 *Buxus* species, which are primarily distributed in tropical and subtropical zones of the world, and potentially to other Buxaceae and non-Buxaceae species. Despite the rapid and ongoing spread of *Cps*, assessments of establishment risk for areas which have not (yet) been invaded are not well developed. Identifying areas which are conducive for establishment by invasive plant

pathogens can guide surveillance efforts and increase the likelihood that pathogens are detected early, which is the most effective and cost-efficient method to avoid the potential ecological, economic, and societal consequences of their spread (Santini et al. 2013, Lovett et al. 2016, Hong 2019a).

In this study, we used multiple climatic suitability modeling approaches to predict the potential distribution of *Cps* at regional and global scales and explore how climatic factors shape its known range limits. Climatic suitability models, also known as ecological niche models, habitat suitability models, bioclimatic envelope models, or climatic envelope models (Elith and Graham 2009), have become an important tool for assessing establishment risk for invasive plant fungal pathogens because their growth and survival is closely related to climatic conditions, particularly temperature and moisture (Magarey et al. 2007, Lantschner et al. 2019). Indeed, the epidemiology of *Cps* is strongly influenced by longer periods of high relative air humidity combined with warm temperatures (Gehesquière 2014, Avenot et al. 2017, LeBlanc et al. 2018). We used a workflow that combined multiple modeling algorithms to reduce predictive uncertainty of single-models, which should enhance the reliability and robustness of predictions and provide independent perspectives into the potential distribution of invasive species (Capinha and Anastácio 2011, Lantschner et al. 2019). First, we used the CLIMEX program (Sutherst and Maywald 1985, Kriticos et al. 2016) to develop a climatic suitability model for *Cps* based on its predicted response to growth- and survival-limiting temperature and moisture factors. The CLIMEX approach is considered process-based because models are typically parameterized using a combination of eco-physiological data (e.g., temperature thresholds for development and survival) and point observations of occupancy or abundance from the species' known geographical distribution (Sutherst and Maywald 1985, Kriticos et al. 2016). CLIMEX is one of the most frequently used climatic suitability modeling tools for invasive pest species, including for plant fungal pathogens (Ireland and Kriticos 2019, Lantschner et al. 2019).

Next, we developed climatic suitability models for *Cps* using multiple correlative modeling algorithms and combined their predictions into an ensemble model to potentially increase predictive performance (Marmion et al. 2009, Shabani et al. 2016, Hao et al. 2020). Correlative climatic suitability models (hereafter correlative models) involve statistically linking spatial climatic data to species location records to estimate the probability of other locations being part of the species distribution (Elith and Graham 2009, Dormann et al. 2012). Correlative

models are thought to be less reliable in predicting a species' potential distribution in novel climates than process-based models, but their advantages include their lower input data needs and generally lower number of parameters (Kearney and Porter 2009, Dormann et al. 2012, Peterson et al. 2015). For example, correlative models only require known distribution data as an input whereas CLIMEX models requires a more extensive baseline knowledge of the species. By joining process-based and correlative approaches in a combined workflow, we strived to incorporate advantages of each approach (Lantschner et al. 2019). Our specific objectives were to identify range-limiting climatic factors for *Cps* using each modeling approach, and to compare the models' predictions of climatic suitability and the overall potential distribution of the pathogen at both regional and global scales. The models developed for this study may help with identifying locations for surveillance to detect *Cps* before it establishes, and they may provide insight into its potential native range, which is hypothesized to be in a host center of diversity for *Buxus* in East Asia, the Caribbean, or Madagascar (LeBlanc et al. 2018, Daughtrey 2019).

Methods

Boxwood blight occurrence records

To fit and validate CLIMEX and correlative models, we compiled 292 occurrence records for *Cps* from 24 countries, which spans the entire known distribution of the pathogen (Europe, Asia, New Zealand, and North America; Appendix 1, Supporting information). Occurrence records were derived from peer-reviewed literature, theses, reports, media sources (e.g., online news articles), the Global Biodiversity Information Facility (2nd April 2021; GBIF Occurrence Download https://doi.org/10.15468/dl.44z8yr), CERIS Pest Tracker (https://pest.ceris.purdue.edu/), the Agricultural Research Service Fungal Database (https://nt.ars-grin.gov/fungaldatabases/), and personal communications. We excluded any record collected from garden centers and/or newly established plantings with boxwood plant stocks originating from another state. Ideally, positive confirmations of *Cps* should be based on both morphological and laboratory-collected data (e.g., genetic and physiological characterization) because some symptoms of boxwood blight overlap somewhat with those of other boxwood diseases (Daughtrey 2019). For several *Cps* records, confirmations were based only on morphological data, or the source did not provide any information on the confirmation process.

However, these records were within or close to areas where *Cps* is known to occur, which suggests the species was correctly identified. Most records for the United States (101/156 = 65%) were spatially resolved only to the county level due to confidentiality concerns, whereas all other records were resolved to at least the city level.

CLIMEX model

The CLIMEX model for *Cps* was generated using CLIMEX version 4.0 (Kriticos et al. 2016). CLIMEX uses a re-formatted version of the CliMond dataset (Kriticos et al. 2012), which is comprised of 35 Bioclim variables for the 1961–1990 time period (https://www.climond.org/). CLIMEX data have a 10′ resolution (*ca.* 55 km^2 at the equator) spatial resolution, which is appropriate given that most records from the United States were spatially resolved only to county level. Eco-physiological information for parameterizing a CLIMEX model for *Cps* was derived from published studies on the impacts of temperature and moisture on the development and survival of the vegetative growing stage as well as the more stress-tolerant microsclerotia stage, which can remain dormant on soil surfaces for months or even years (Henricot et al. 2008, Dart et al. 2015). We fine-tuned CLIMEX parameters by fitting the model to occurrence records from Europe and western Asia (N = 125), where the species may have had more time to fill its climatic niche compared to more recently invaded regions. Only one parameter was adjusted at a time during this process. We then validated the CLIMEX model by verifying that records from North America (N = 159) and New Zealand (N = 8) fell within climatically suitable areas as defined by the ecoclimatic index, which ranges from 0 to 100 and describes the overall suitability of a location for long-term persistence by a species (Sutherst 2014, Kriticos et al. 2016). The ecoclimatic index integrates the annual growth index, which describes the potential for population growth (also ranging from 0 to 100), with annual stresses that limit survival during unfavorable intervals (cold, heat, dry, and wet stress) and potentially other limiting factors such as diapause. A species is considered to be excluded from locations which have an ecoclimatic index of zero, whereas increasing ecoclimatic index values signify higher potential for growth and survival (Kriticos et al. 2016). We report CLIMEX model parameters for *Cps* in Table 1 and describe how we derived each parameter value in the next two subsections.

Temperature and moisture index parameters

Four temperature index parameters in CLIMEX describe the ability for temperature-driven population growth: DV0 (limiting low temperature), DV1 (lower optimal temperature), DV2 (upper optimal temperature), and DV3 (limiting high temperature). *Cps* may develop at temperatures as low as 5 ºC (Henricot and Culham 2002, Gehesquière 2014, Gehesquière et al. 2016), but we set DV0 to 9 ºC to avoid potential biases resulting from canopy temperatures being lower than estimates from weather stations, which can produce errors in plant disease models (Pfender et al. 2012). We set DV1 and DV2 to 21 and 25 ºC, respectively, because this temperature range is associated with optimal growing conditions in both field and laboratory settings (Henricot and Culham 2002, Gehesquière 2014, Gehesquière et al. 2016, Avenot et al. 2017, Lehtijärvi et al. 2017). We used an upper threshold of 29 ºC because *Cps* colonies exhibit a low growth rate and have irregular and sclerotized morphologies at temperatures ≥ 28 ºC (Gehesquière 2014, Gehesquière et al. 2016, Avenot et al. 2017). Our unpublished re-analysis of Gehesquiere (2014) data indicated that 500 degree-hours during continuous leaf wetness would cause between *ca.* 10-50% infection for *B. sempervirens* and *B. s.* var 'Suffruticosa', which is equivalent to 20 degree-days. However, CLIMEX has no way to integrate moisture with degree-day calculations, so we used a 10× higher value of 200 as a rough stand-in for the degree-days per generation parameter (PDD). The PDD value therefore has no true meaning with regard to actual infection conditions because it accounts only for favorable temperatures.

CLIMEX describes the overall moisture characteristic of a location using estimates of soil moisture, which combine the interactions of temperature, rainfall and evapotranspiration. While precipitation and dew point are the primary moisture drivers of *Cps* growth (Shishkoff and Camp 2016, Avenot et al. 2017, LeBlanc et al. 2018), the use of soil moisture in CLIMEX should capture the species' response to its moisture environment in a broad sense. Four soil moisture (SM) index parameters describe the influence of moisture on population growth: SM0 (limiting low moisture), SM1 (lower optimal moisture), SM2 (upper optimal moisture), and SM3 (limiting high moisture). For each SM parameter, a value of 0 indicates no soil moisture, a value of 0.5 indicates soil moisture content is 50% of capacity, a value of 1 indicates that soil moisture content is 100% of capacity, and a value > 1 indicates a water content greater than the soil holding capacity (Kriticos et al. 2016). We set SM0 to 0.2, which is higher than the permanent wilting point of plants in CLIMEX (SM0 = 0.1), because pathogens including *Cps* require free water for parts of their lifecycles. We set SM1 to 0.7 because using higher values resulted in

certain occurrence records from more inland areas of the Black Sea and Caspian Sea regions being excluded (i.e., ecoclimatic index = 0). The upper optimal value (SM2) was set to 1.7 to ensure that wet conditions were suitable, and the upper threshold (SM3) was set to 3 to remove any constraints on growth related to very high rainfall.

Temperature and moisture stress parameters

The cold and heat stress thresholds (TTCS and TTHS, respectively) in CLIMEX define the temperature below (TTCS) or above (TTHS) which stress begins to accumulate according to a weekly rate (Kriticos et al. 2016). For example, if the average weekly maximum temperature (T_{max}) exceeds TTHS, then heat stress = (T_{max} – TTHS) × THHS, where THHS is described by the slope of the relationship between weekly heat stress and average weekly T_{max}. The threshold temperature function in CLIMEX has a multiplicative factor (referred to as "week number") that causes stress to accumulate exponentially during consecutive weeks. To help identify appropriate TTCS and THHS values, we extracted minimum temperature of the coldest week data (bio6) and maximum temperature of the warmest week (bio6) data from the CliMond dataset for *Cps* occurrence records from Europe and western Asia. According to this analysis, all localities in the coldest parts of *Cps*'s distribution, which occur in northern Europe and high-elevation parts of Georgia, were in areas where weekly minimum temperatures were ≥ –8 ºC. This finding is consistent with temperature limits of the most cold tolerant boxwood varieties, which are almost impossible to grow in areas where temperatures drop below –10 ºC (United States Department of Agriculture 1976), and with laboratory studies of *Cps* microsclerotia survival (Shishkoff and Camp 2016, Yang and Hong 2018). We set TTCS to –10 ºC and adjusted the cold stress rate (THCS) to ensure that the coldest localities for *Cps* in Europe and western Asia fell within areas where the ecoclimatic index exceeded zero. Additionally, we considered maps of the northern range limit for European boxwood *B. sempervirens* (Pojark.) in Norway, which is largely confined to districts south of 62º N (Salvesen and Kanz 2009).

We set TTHS to 32 ºC and adjusted the heat stress accumulation rate (HDS) so that records from the hottest part of *Cps*'s distribution, which occur in northern Iran along the Caspian Sea (Mirabolfathy 2013, Khazaeli et al. 2015), had ecoclimatic index values exceeding zero. Microsclerotia have been shown to survive at 40° C for at least 24 hours (Yang and Hong 2018); however, other data sources suggest that heat stress accumulates at lower temperatures.

An upper lethal temperatures of 33 °C has been suggested by Henricot and Culham (2002) based on a laboratory study of conidial growth (Henricot and Culham 2002), and by Hagan and Conner based on field reports. Additionally, microsclerotia died after two to five months at 30 ºC under laboratory conditions (Shishkoff and Camp 2016), which, if translated to field conditions, would be slightly cooler in the soil under a canopy than in weather shelters. All but a single locality record for *Cps* in Europe and western Asia occurred in areas where weekly maximum temperatures fell below 32 ºC, which provides further evidence that this temperature is an appropriate heat stress threshold.

Whereas extremely low soil moisture reduces survival of *Cps* (Shishkoff and Camp 2016, Avenot et al. 2017), excessive moisture is not known to be detrimental to survival of the pathogen. We set the dry stress threshold (SMDS) to 0.2 and weekly dry stress rate (HDS) to –0.001 because this contributed to the exclusion of the species (ecoclimatic index = 0) from relatively arid areas beyond the Black Sea and Caspian Sea regions, where boxwood does not occur (Hūšang 1989, Lehtijärvi et al. 2017). Conversely, we used a relatively high wet stress threshold (SMWS) of 3.0 and set the rate of wet stress accumulation (HWS) to 0.005. We did not apply the hot-dry (interaction) stress parameter in CLIMEX because preliminary analyses indicated that it did not assist in modeling the potential distribution.

Irrigation

To explore how supplemental irrigation may influence climatic suitability and the potential distribution of *Cps*, we ran the CLIMEX model both with and without an option to apply 'top-up' amounts irrigation (rainfall) of 2.5 mm day^{-1} during the summer (Kriticos et al. 2016). Summer irrigation is regularly used in horticultural settings where boxwood is grown (United States Department of Agriculture 1976), and it can play a key role in *Cps* growth and survival by increasing the humidity to levels conducive for sporulation and infection (Gehesquière 2014, Bartíková et al. 2020b). Henceforth the model which did not include irrigation is simply referred to as the "CLIMEX model."

Correlative models

We generated correlative models for *Cps* in the *ENMTML* R package v. 1.0.0 (de Andrade et al. 2020) in R version 4.0.5 (R Development Core Team 2021). *ENMTML* provides a suite of

functions to preprocess locality and environmental input data, fit models using a variety of algorithms, evaluate model performance for each algorithm, and combine model outputs to produce an ensemble model (de Andrade et al. 2020). We fit models using occurrence records from Europe, western Asia, and North America because prediction accuracy of correlative models is often higher when a larger proportion of the realized climatic niche is sampled (Beaumont et al. 2009, Taylor and Kumar 2012, Pili et al. 2020).

Two filtering steps were taken on records to reduce biased geographic sampling, which can strongly affect the predictive performance of correlative climatic suitability models that use presence-only data (Veloz 2009, Kramer-Schadt et al. 2013). First, we reduced the effects of clustered sampling by implementing the "pp.subsample" function in the *spatialEco* R package v. 1.3.7 (Evans 2021), which created a subsample of 80% of *Cps* records for both regions based on the expected spatial intensity function of the observed data. Second, we thinned records within *ENMTML* using the "CELLSIZE" method of the "thin_occ" function in the *spThin* R package v. 0.2.0 (Aiello-Lammens et al. 2015), which removes records that occur within a distance of two cells. This process resulted in 67 records for Europe and western Asia (67/163 = 41%), and 96 records for North America (96/163 = 59%). Maps presenting the full and subsampled occurrence records for both regions are presented in Fig. S1 (Supporting information).

Twenty-seven bioclimatic variables from the CliMond dataset were used to generate correlative SDMs (Kriticos et al. 2012). The first 19 bioclimatic variables (bio1-bio19) are derived from the WorldClim data set and represent annual, weekly (interpolated from monthly), and seasonal trends and extremes in temperature and precipitation (Hijmans et al. 2005). Eight bioclimatic variables that describe weekly, quarterly and annual indices of soil moisture (bio28-bio35) were also included because considering soil moisture should increase comparability of model predictions between CLIMEX and correlative models. We cropped bioclimatic layers to areas where *Cps* could reasonably disperse to because restricting the theoretically accessible area used for model fitting can significantly improve model performance (Cooper and Soberón 2018). This included areas between 25.5 ºN and 25.5 ºS in both regions, between 170 ºW and 51 ºW in North America (conterminous United States and southern Canada), and between 12 ºW and 61.9 ºE in Eurasia (western Europe to the eastern border of Iran).

A principal component analysis (PCA) was conducted based on the correlation matrix of the 27 cropped climate variables to reduce variable collinearity, which can reduce uncertainty of

correlative models and increase performance of models projections into new regions (Veloz 2009, Dormann et al. 2013, Petitpierre et al. 2017, De Marco and Nóbrega 2018). We produced a dataset comprised of six principal components (PCs) that explained at least 95% of the total variance (De Marco and Nóbrega 2018) using the "rasterPCA" function in the *RSToolbox* R package v. 0.2.6 (Leutner and Horning 2017). The first and second PC axes explained the highest proportion of the total variance (52.2% + 27.3% = 79.5%) and had strongest contributions from moisture and temperature variables, respectively (Table 2). The first PC axis (PC1) had a strong positive loading for soil moisture seasonality (bio31) and strong negative loadings for precipitation and soil moisture during warm seasons (bio18 and bio34, respectively), reflecting lower warm season moisture and higher moisture seasonality at positive PC1 scores (Table 2 and Fig. S2, Supporting information). The second PC axis (PC2) had strong positive loadings for temperatures during cold seasons (bio6 and bio11) and strong negative loadings for temperature seasonality and annual range (bio4 and bio7, respectively), reflecting lower winter temperatures and higher temperature seasonality at positive PC2 scores. PC axes 3 through 6 explained the remaining 16.3% of total variance and were primarily related to temperatures during warm and wet seasons (PC3), wet season precipitation (PC4), diurnal cold and wet season temperature range and soil moisture (PC5), and dry season precipitation and precipitation seasonality (PC6).

Six different algorithms were used to fit correlative models in *ENMTML* and assess variable importance. These included: boosted regression tree (Elith et al. 2008), generalized additive models (Guisan et al. 2002), Gaussian process usage (Golding and Purse 2016), Maxent with applied linear and quadratic features ("Maxent simple") (Phillips et al. 2006, 2017), random forests (Prasad et al. 2006), and support vector machine (Guo et al. 2005). *ENMTML* sources modeling algorithm functions from multiple different R packages and uses default settings (Table S1, Supporting information) unless the user manually edits the program. We applied default settings for all algorithms except for Maxent, in which we increased the regularization multiplier parameter from one (default) to four to avoid model overfitting (Phillips et al. 2006). We used the three-step pseudo-absence selection method of Senay et al. (2013) to allocate pseudo-absences, wherein a sample of environmentally dissimilar locations within a 400 km buffer around occurrence records were identified and then sampled using k-means clustering. Information on the individual R package repositories and settings used for each modeling algorithm is presented in Table S1, Supporting information.

In the post-processing stage of *ENMTML*, we evaluated model performance for each algorithm and produced an ensemble model from single-model outputs. Model performance was assessed using 50 bootstrapped replicates for each algorithm, with a random 70% subset of records used to train the model and 30% reserved for validation. Model replicates were then projected at a global scale using the same climatic PC predictors. We evaluated SDMs using the area under the receiving operating characteristic curve (AUC), true skill statistics (TSS), Kappa, Jaccard, Sørensen, Boyce, and F-measure on presence-background data (F_{pb}) metrics (Boyce et al. 2002, Allouche et al. 2006, Li and Guo 2013, Leroy et al. 2018). Similarity indices from community ecology (Jaccard, Sørensen and F_{pb}) may provide better estimations of model discrimination capacity than metrics which depend on prevalence (the proportion of sites where the species is present) including AUC and Kappa (Allouche et al. 2006, Li and Guo 2013, Leroy et al. 2018).

An ensemble model was produced by calculating a weighted mean of suitability predictions (probability of occurrence) of the best models across all algorithms, defined as those which had an F_{pb} metric exceeding the average for all models (Thuiller 2004). Additionally, we overlaid predictions of presence-absence produced by the six algorithms to compare delimitations of the potential distribution. The maximum TSS threshold, which maximizes the sum of sensitivity (proportion of correctly predicted observations of species presence) and specificity (proportion of correctly predicted observations of species absence), was used to produce presence-absence predictions because it may have higher accuracy than other threshold methods (Liu et al. 2005, França and Cabral 2019). We tested the climatic similarity between the model calibration and global projection areas using a mobility-oriented parity (MOP) analysis (Owens et al. 2013) to identify potential regions where strict extrapolation occurred, wherein climatic conditions are outside of the range of conditions in the calibration area. Model extrapolation into new regions or climate change scenarios may change the correlation structure between parameters and thus lead to unreliable predictions when projected outside the environmental space (Dormann et al. 2013, Owens et al. 2013, Petitpierre et al. 2017). The MOP analysis sampled 10% of reference points from the environmental space of the calibration area and was conducted within *ENMTML* using the “MOP” function in *kuenm* R package v. 1.1.7 (Cobos et al. 2019). Finally, we produced consensus maps depicting areas of overlap in the potential distribution as estimated by presence-absence predictions of the ensemble correlative

model and the CLIMEX model. In theory, an ecoclimatic index which exceeds 0 indicates a potential for establishment (Kriticos et al. 2016); however, we defined the potential distribution in CLIMEX as areas which had an ecoclimatic index of at least 10 because most occurrence records (286/292 = 98%) met this criterion.

Results

Model evaluation and variable importance in correlative models

Validation analyses indicated very good performance of the CLIMEX model and correlative models. Of the 124 occurrence records from Europe and western Asia used for fine-tuning CLIMEX parameters, only one fell within an unsuitable location (i.e., ecoclimatic index = 0). All occurrence records from North America and New Zealand were in areas that CLIMEX predicted to be climatically suitable (average ecoclimatic index = 24, range = 10 to 60), which provided validation of good model fit. Evaluation metrics for the final ensemble correlative model were very high (Table 3): the AUC, TSS, Kappa, Jaccard, Sørensen, and Boyce metrics exceeded 0.99 (values > 0.90 are considered excellent performance) and F_{pb} was 1.99 ($F_{pb} = 2 \times$ Jaccard). Metric values for single models across 50 repetitions were also high, with an average of 0.998 for AUC (range = 0.996–1), 0.981 for Kappa (range = 0.974–0.992), 0.981 for TSS (range = 0.975–0.992), 0.981 for Jaccard (range = 0.975–0.992), 0.991 for Sørensen (range = 0.987–0.996), and 1.96 for F_{pb} (range = 1.95–1.98). The PC2 variable contributed most strongly (average = 47%) to correlative models (Table 4), indicating an important role for cold temperatures and temperature seasonality in shaping the distribution of *Cps*. The PC1 variable provided the next highest contribution to correlative models (average = 24.3%), indicating that warm season moisture and moisture seasonality (PC1) are also important range-limiting factors. On average, the remaining PC variables had relatively low contributions (PC3 = 8.5%, PC4 = 4.8%, PC5 = 9.8%, PC6 = 5.6%).

Climatic suitability for and potential distribution of Cps *in Europe and western Asia*

CLIMEX and the ensemble correlative model predictions of climatic suitability and the potential distribution for *Cps* in Europe and western Asia were mostly concordant (Fig. 1). CLIMEX predicted the highest ecoclimatic and population growth index values in the Atlantic region of

western Europe, coastal areas of southern Europe, and the Black and Caspian Sea regions of western Asia (Figs 1A and 2A, respectively), which is consistent with the ensemble correlative model's predictions of high climatic suitability for these areas (Fig. 1C). Consequently, these regions were included in the potential distribution according to both models (Fig. 1D). In general, the models predicted lower climatic suitability throughout most of central and eastern Europe, but these areas were nonetheless included in the potential distribution. CLIMEX's estimate of the potential distribution extended farther east than that of the ensemble correlative model to include all of the Baltic states and Belarus, a greater area of Ukraine, and the border region of Russia. However, predictions of suitability and the potential distribution in these regions varied among the six correlative modeling algorithms, which indicates model uncertainty (Figs S3 and S4, Supporting information). For example, the Gaussian process and support vector machine algorithms predicted a larger extent of climatically suitable area in eastern Europe than other algorithms.

Temperature and aridity were both important range-limiting factors for *Cps* in Europe and western Asia. According to CLIMEX, cold stress is predicted to constrain *Cps* to latitudes below *ca.* 60° N in Europe, and it would exclude the species from western Russia except for the southernmost regions (Fig. 2B). Conversely, a combination of heat and dry stress in Iran and countries on the eastern edge of the Caspian Sea (e.g., Turkmenistan, Kazakhstan) is predicted to limit the species to predominantly southwestern areas of the Caspian Sea region (Figs 2C, D). Heat and dry stress are also predicted to exclude *Cps* from most of southern Spain and surrounding non-coastal areas of northwestern Africa. Employing the irrigation option in CLIMEX resulted in increases in climatic suitability along the species' predicted range throughout Europe and western Asia (Fig. 1B), which subsequently resulted in an expansion in the potential distribution in northern Europe (Sweden and Finland), southern Europe (e.g., Greece), eastern Europe (Ukraine), western Russia, Turkey, and the Caucasus (e.g., Armenia and Azerbaijan).

Climatic suitability for and potential distribution of Cps *in North America*

Overall, predictions of climatic suitability and the potential distribution estimated by CLIMEX and the ensemble correlative model were concordant for North America (Fig. 3). Both models predicted climatically suitable conditions throughout most of eastern United States, whereas

suitable conditions in the western United States were almost entirely limited to the Pacific coast region (Fig. 3A–C). CLIMEX predicted the highest ecoclimatic and population growth index values in the eastern United States particularly in states along the east coast and Gulf coast (Figs 3A, 4A). Several southeastern and midwestern states where *Cps* is not known to be established were predicted to be climatically suitable for this pathogen. These include Arkansas, Missouri, Illinois, and Indiana. In the western United States and southern British Columbia, the potential distribution included western Oregon and Washington, coastal areas of California and southern British Columbia, the Sierra Nevada Mountain range (California), and a small area of the northern Rocky Mountains in Idaho and British Columbia. Major portions of the Great Plains, Intermountain West and Southwest were excluded from the potential distribution even in the CLIMEX model that included summer irrigation (Fig. 3B, D). The northernmost parts of the potential distribution were limited to coastal areas of the Pacific (British Columbia) and Atlantic (Quebec, Novia Scotia, and New Brunswick).

The ensemble correlative model predicted a somewhat larger potential distribution for *Cps* in eastern North America than the CLIMEX model. Specifically, it included more inland parts of the Southeast and higher latitude parts of the Northeast and southern Canada (Fig. 3D). For example, the potential distribution extended farther west in the southeastern United States and included eastern Texas and Oklahoma, and it extended farther north in eastern North America and included all northeastern states and southern Quebec and Ontario. Predictions of climatic suitability and presence for these areas were mostly consistent across individual correlative modeling algorithms (Figs S4 and S5, Supporting information).

According to CLIMEX, cold stress was the primary range-limiting factor for *Cps* in North America (Fig. 4B), although arid conditions in the Intermountain West and hot temperatures in the South limited the pathogen's distribution in those areas (Figs 4C, D). Cold stress excluded the species from high-elevation areas in the Intermountain West (most of the Rocky Mountains), from northern parts of the Northeast (northern New York and most of Vermont, New Hampshire, and Maine) and the Midwest (most of Wisconsin and all of North Dakota, South Dakota, and Minnesota), and from Canada and Alaska except for some coastal areas of the Pacific. Estimates of population growth for North America (Fig. 4A) indicate that *Cps* populations could grow in several areas which were excluded by cold stress, a finding which suggests that populations could at least temporarily establish during favorable seasons. For

example, population growth was high in Wisconsin, New England, and southern parts of Ontario and Quebec; however, cold stress is predicted to prevent overwintering survival throughout most of these areas. Similarly, heat stress contributed to the exclusion of *Cps* in eastern Texas despite high population growth rates. Population growth and survival were both low across the Intermountain West primarily due to insufficient moisture, and heat stress and dry stress contributed to exclusion of the pathogen from much of the Southwest including western Texas. Employing the irrigation option in CLIMEX resulted in increases in climatic suitability throughout much of the western United States (Fig. 3B); however, increases were insufficient for the inclusion of the Intermountain West and Southwest in the potential distribution.

Global climatic suitability for and potential distribution of Cps

Ensemble correlative model projections at a global scale were only partially consistent with the CLIMEX model (Figs 5 and 6). Both modeling approaches predicted highly suitable conditions in New Zealand, where *Cps* has been reported on both the North and South Island (Appendix 1, Supporting information), and throughout southeastern China, Japan, southern Australia, South Africa (coastal areas), Uruguay, and parts of Brazil, Argentina, Paraguay, and southern Chile (Fig. 5). Additionally, the ensemble correlative model predicted unsuitable conditions in most of the same areas where CLIMEX predicted unsuitability due to high levels of cold stress (e.g., in northern Asia; Fig. S6, Supporting information). While concordant predictions of climatic suitability for these regions translated to broad overlap in estimates of the potential distribution (Fig. 6), CLIMEX predicted higher climatic suitability and a larger potential distribution in other regions of the world. Model predictions were particularly discordant in equatorial (tropical) regions of South Asia, Africa, and South and Central America. For example, most high elevation areas of Africa and South Asia that were included the potential distribution according to CLIMEX had low or zero climatic suitability in the ensemble correlative model, whereas lower elevation regions that were included in the potential distribution by the ensemble model such as in India and the Indochina peninsula were unsuitable in the CLIMEX model (Fig. 5) due to heat stress (Fig. S6, Supporting information). The MOP analysis of climatic PC predictors used for the ensemble correlative model revealed high levels of similarity in climate between the calibration and projection area in temperate regions of the world (MOP index ≥ 0.9), but dissimilarity was higher in equatorial regions, particularly in parts of Southeast Asia and South

America (Fig. 7). This finding indicates that portions of environmental space in equatorial regions may be within the range of individual variables but they represent new combinations of predictors, which suggests that predictions there may be unreliable (Zurell et al. 2012, Owens et al. 2013). Employing the irrigation option in CLIMEX resulted in only marginal increases in the global potential distribution, mostly in coastal areas of arid parts of South America (e.g., Chile and Peru), Africa (e.g., Morocco and Namibia), and southern Australia.

Discussion

This study used both process-based CLIMEX and correlative models to assess the risk for *Cps*, a highly invasive plant pathogen, to establish at local, regional and global scales. This assessment can help guide the development of local and regional phytosanitary protocols for preventing further spread of the pathogen, prioritizing global surveillance efforts for more effective early detection, and planning for eradication, containment and management where accidental introductions do occur. These three steps are critical to preventing accidental introductions of *Cps* to and becoming established in predicted high risk areas where it is not yet present (Daughtrey 2019, Hong 2019b). They are also crucial to preventing boxwood blight from becoming rampant in areas where this invasive pathogen is at its early stages of establishment (Henricot 2006). *Cps* has spread rapidly, as evidenced by its invasion of 24 countries across three distant regions (Europe and western Asia, New Zealand, and North America) in less than 30 years (Palmer and Shishkoff 2014, LeBlanc et al. 2018, Daughtrey 2019). Preventing its accidental introduction to and establishment in new areas and mitigating its local spread are both pivotal to safeguarding global boxwood crops, plantings, and forests (Daughtrey 2019, Hong 2019b).

All models performed very well and were mostly consistent in their predictions for the calibration area (i.e., Europe, western Asia, and North America). The process-based CLIMEX model correctly predicted climatically suitable conditions at validation localities for *Cps* in North America and New Zealand, and the six individual correlative models and ensemble model had very high evaluation metrics for the calibration area. Cold temperatures were a major range-limitation at higher latitudes and elevations, as evidenced by the absence of the species from northern areas which have high levels of cold stress in the CLIMEX model, and by the strong

contribution of the cold-temperature related PC predictor (PC2) to correlative models. Moisture during warm seasons was also a major range limiting factor, as demonstrated by increases in climatic suitability and the potential distribution which occurred when implementing the summer irrigation option in CLIMEX, and by the strong contribution of the PC predictor (PC1) related to warm season moisture and moisture seasonality to correlative models. Hot temperatures, often in combination with arid conditions, play a range-limiting role for *Cps* predominantly in the southern regions of western Asia (e.g., northern Iran) and in the United States particularly in the Southwest.

Climatic suitability for and potential distribution of Cps *in Europe, western Asia, and North America*

Some of the highest levels of climatic suitability according to the CLIMEX and ensemble correlative model occurred in western Europe, western Asia (Black and Caspian Sea regions), and the east coast of the United States, a finding which is consistent with the widespread presence of *Cps* in these regions. Oceanic climates in these areas has probably facilitated the pathogen's invasion because few gaps in precipitation and high humidity over the year combined with warm-to-hot summer temperatures creates conducive conditions for infections (Fig. 8) (Gehesquière 2014, Daughtrey 2019). In the eastern United States, *Cps* is particularly prevalent in the Mid-Atlantic and northern parts of the Southeast; however, there are relatively few reports of the pathogen from Florida and the Deep South (southernmost states in the Southeast), despite the inclusion of most of these regions in the potential distribution. For example, boxwood blight has not been reported beyond two locations in the Tallahassee area of northern Florida in 2016 where contaminated stock plants were received and then eradicated in 2016 (Iriarte et al. 2016), and to date there have been no positive reports for Texas, Louisiana, and Mississippi (Hall 2021). According to CLIMEX, hot temperatures reduced climatic suitability throughout Florida except for along coastlines and from the Deep South except for northern parts of some states (e.g., northern Alabama and Georgia), which may explain the paucity of reports from these areas. Hagan and Conner (2013) posited that disease development on container or field stock in Alabama would most likely occur during extended periods of wet weather in mid-fall into mid-spring because temperatures would be more ideal for growth than during the summer. Additionally, shade can reduce temperatures and create humid conditions that may create more

favorable conditions for infections in hot environments (Bush et al. 2016, Daughtrey 2019). Additional data on the pathogen's ability to survive prolonged heat, particularly in the more heat-resistant microsclerotia form (Shishkoff and Camp 2016, Miller et al. 2018, Yang and Hong 2018), could help resolve whether it may establish in parts of the Deep South which may have ideal growing conditions during cool seasons.

Many areas with Mediterranean climates including those in southern Europe and the Pacific coast region of the United States were included in the potential distribution according to both modeling approaches, but *Cps* has a limited presence in these regions to date. In southern Europe, *Cps* has been reported on *B. sempervirens* 'Suffruticosa' in nurseries or gardens from only a handful of localities in northwestern Spain (Pintos Varela et al. 2009), southern France (Saurat et al. 2012), northern Italy (Saracchi et al. 2008), and Croatia (Cech et al. 2010). The pathogen has seemingly had opportunities to invade southern Europe given its rapid expansion throughout other parts of the continent beginning in *ca.* 1994 (LeBlanc et al. 2018, Daughtrey 2019). Host availability is likely not an issue because boxwood is commonly grown in gardens and landscapes throughout southern Europe, and native populations of *B. sempervirens* and *B. balearica* occur in pockets in northern Africa (Morocco and Algeria), central France, the southern European peninsulas (Iberian, Italian and Balkan), certain Mediterranean Islands, and Turkey (Di Domenico et al. 2012, Caudullo et al. 2017). In the western United States, *Cps* has been documented only in a handful of locations in western Oregon and the San Francisco Bay area despite having a potential distribution which encompasses Mediterranean climates throughout the region, including the entire California coast, parts of the Sierra Nevada Mountain range, and areas west of the Cascade Mountains in Oregon and Washington. Long warm-to-hot dry summers and cool wet winters which characterize Mediterranean climates may hinder long-term establishment of *Cps* because optimal conditions for growth that transpire during warm and wet weather occur too infrequently (Fig. 8). Applying the summer irrigation option in the CLIMEX model resulted in an increase in suitability throughout southern Europe and areas with Mediterranean climates in the western United States, a finding which is consistent with observations that outbreaks in Oregon and California are often associated with summer irrigation (J. Weiland, pers. comm.) or unusually wet spring and summers (Blomquist et al. 2018). Thus, regions with Mediterranean climate will likely be at higher risk of establishment if boxwood is irrigated during periods of optimal temperatures for *Cps* development, or during relatively wet

559 years. Overhead irrigation in particular facilitates boxwood blight outbreaks because it creates
560 higher relative humidity and exposes leaf surfaces to longer periods of wetness (Gehesquière
561 2014, Bartíková et al. 2020b, 2020a).
562 Climatic suitability tended to be lower in regions with humid continental climates
563 compared to those with oceanic climates, despite the inclusion of many of these areas in the
564 potential distribution. In humid continental parts of Europe, which includes most of eastern
565 Europe and parts of Ukraine and Russia, optimal conditions for infections (warm and wet
566 weather) may occur too infrequently owing to long, cold winters and warm-to-hot, dry summers.
567 The only reports of the pathogen from these regions have come from nurseries and gardens in the
568 Czech Republic (Safránková et al. 2012, Bartíková et al. 2020a) and a single nursery in western
569 Ukraine (Matsiakh 2016). The common element of diseased boxwood in gardens in the Czech
570 Republic was the use of irrigation systems or partial-shade conditions, which created higher
571 humidity and exposed leaves longer periods of wetness (Bartíková et al. 2020a). Implementing
572 the summer irrigation option in CLIMEX increased suitability throughout central and eastern
573 Europe and resulted in an expansion of the potential distribution in western Russia, Ukraine,
574 Turkey and the Caucasus, which provides additional evidence that irrigation will likely increase
575 the risk of establishment of *Cps* in these regions.
576 As with Europe, climatic suitability tended to be lower in humid continental regions of
577 North America that were included in the potential distribution; however, cool temperatures rather
578 than aridity likely explain this finding. According to CLIMEX, cold stress lowered climatic
579 suitability throughout much of non-coastal New York, New England, and southeastern Canada,
580 which is consistent with an absence of *Cps* from these areas and with lower suitability predicted
581 by the ensemble correlative model. In the midwestern United States, *Cps* has a limited presence
582 despite the growing number of reports of the pathogen for this region, including from Missouri
583 (2014), Kansas (2014), Illinois (2016), Indiana (2018), Arkansas (2019), Michigan (2018), and
584 Wisconsin (2018). Nevertheless, economic damages to the horticultural industry in the Midwest
585 could be significant if *Cps* takes hold because this region is one of the top four regions in inter-
586 regional trade of boxwood (Hall et al. 2021), which supports the need for boxwood producers
587 and users to be vigilant in watching for infections and quickly eradicating the pathogen when it is
588 found (Hong 2019a). Our models indicate that cold temperatures will likely prevent
589 establishment in northern Minnesota, northern Wisconsin, most of Nebraska, North Dakota, and

South Dakota. *Cps* was found in North Dakota in 2019 on contaminated stock plants that were received from Ohio, but it has not been found in landscape settings where it could potentially be exposed to winter conditions (Charles Elhard, pers. comm.). Future outbreak reports from areas which are predicted to be too cold for establishment should be followed closely to assess the ability of *Cps* to overwinter. For example, soil or snow cover may offer protection to overwintering microsclerotia that may allow the pathogen to survive in areas which are predicted to be unsuitable by our models.

Areas of Europe, western Asia, and North America which have arid or semi-arid climates had some of the lowest levels of climatic suitability, and will therefore be at relatively low risk of establishment at least in the absence of supplemental moisture. Range expansion of *Cps* in northern Europe and Russia will likely be prevented by cold temperatures; however, aridity often combined with hot temperatures may play a large role in limiting the pathogen's expansion at its eastern range edge (Caspian Sea region) and southern range edge (Spain, Turkey and the Caspian Sea region). In North America, cold temperatures were predicted to exclude *Cps* from most of western Canada and the Rocky Mountains region; however, aridity in the Intermountain West and Southwest played the most significant role in restricting the pathogen's potential distribution in the western United States. Implementing the irrigation option in CLIMEX did not appreciably increase climatic suitability in the Intermountain West or Southwest, which suggests that infections there may only be possible in highly irrigated settings, and potentially in shaded areas during the hot season. With the exception of New Mexico, states in these regions have low rankings for production and total sales of boxwood (Hall et al. 2021), which could further limit the chance for *Cps* to establish there.

Global climatic suitability for and potential distribution of Cps

Maps of climatic suitability and the potential distribution for *Cps* indicate that most regions of the world where *Buxus* and its congeners (*Didymeles*, *Haptanthus*, *Pachysandra*, *Sarcococca*, and *Styloceras*) are native are at risk of establishment. Most of the Buxaceae species are tropical or subtropical, with native ranges that include western and southern Europe, southwest, southern and eastern Asia, Africa, Madagascar, northernmost South America, Central America, Mexico and the Caribbean (Köhler and Brückner 1989, Balthazar et al. 2000, Köhler 2014). The CLIMEX and ensemble correlative models included much of eastern Asia and the

Himalayas in the potential distribution, which are home to *ca.* 40 species of *Buxus* (Köhler and Brückner 1989), four species of *Pachysandra*, and 11 species of *Sarcococca* (Balthazar et al. 2000). According to CLIMEX, the potential distribution in the Neotropics included the Andes region, where all five species of *Styloceras* Kunth ex A. Juss. are endemic (Balthazar et al. 2000), and it overlapped with at least some of the *ca.* 50 species of *Buxus* native to Central America and the Caribbean, such as in Mexico, Guatemala, Cuba, Hispaniola, and Puerto Rico (Köhler and Brückner 1989, Gutiérrez 2014, Köhler 2014). For Africa, both modeling approaches included a narrow band of the South African coast which has endemic *Buxus* (Friss 1989) in the potential distribution, and CLIMEX included additional areas where *Buxus* species occur including in Madagascar (nine species) (Schatz and Lowry 2002) and in western and eastern Africa (e.g., in Ethiopia, Kenya, Tanzania, and Angola)(Friss 1989). An overall lack of comprehensive and current maps that depict the ranges of Buxaceae species hinders making detailed assessments into the extent of overlap with the potential distribution of *Cps*. Nonetheless, our broad-scale assessment indicates the potential for the pathogen to expand its range globally.

Preventing the establishment of *Cps* in regions with native boxwood is important because the pathogen can clearly cause ecological damage to affected ecosystems. Studies of *Cps* in native stands of *B. sempervirens* subsp. *colchica* in Georgia and *B. sempervirens* subsp. *hyrcana* in the Caspian Hyrcanian forests of northern Iran revealed rapid and intensive defoliation of boxwood plants of different ages, with complete defoliation occurring in up to 90% of some populations in just one year after positive detection of boxwood blight (Mirabolfathy 2013, Matsiakh 2016). Infected plants are also vulnerable to attacks by secondary opportunistic pathogens that can lead to eventual death (Matsiakh 2016). A literature survey showed that a loss of native boxwood in Europe and the Caucasus could lead to reductions in soil stability and subsequent declines in water quality and flood protection, and to declines in *Buxus*-associated biodiversity including at least 63 potentially obligate species of lichens, fungi, chromista and invertebrates (Mitchell et al. 2018). Currently there is no effective control for boxwood blight in forests because removing infected plants or applying fungicides across large areas is infeasible (Matsiakh 2016, Patarkalashvili 2017). Early detection of *Cps* will therefore be the most economical and effective method to prevent additional invasions in areas with susceptible native species.

The invasion of *Cps* could be particularly devastating to species which are vulnerable both in terms of their conservation status and their susceptibility to infection. Many *Buxus* species are already threatened or endangered because of small and isolated distributions resulting from natural causes such as island endemism and post-glacial climate change (Di Domenico et al. 2012, Gutiérrez 2014), anthropogenic disturbances such as deforestation and over-harvesting of wood (Mitchell et al. 2018), and invasions of non-native pests such as the box tree moth *Cydalima perspectalis* (Walker, 1859) in Europe and western Asia (Matsiakh 2016, Patarkalashvili 2017, Matsiakh et al. 2018, Panahi et al. 2021). For example, most of the *Buxus* species native to tropical America are endemic to single islands in the Caribbean (Köhler and Brückner 1989), 37 of which occur in Cuba alone (Gutiérrez 2014, Köhler 2014). None of the Buxaceae species tested to date are completely immune to boxwood blight infections, although severity of disease varies widely across *Buxus* species and cultivars (Henricot et al. 2008, Shishkoff et al. 2015, LaMondia and Shishkoff 2017), and it appears to be low in pachysandra (*Pachysandra*) and sweet box species (*Sarcococca*) species (Ryan et al. 2018, Kong and Hong 2019). Susceptible species which have at least partially overlapping native ranges with the potential distribution of *Cps* include *B. sempervirens* and subspecies (southern Europe and the Black and Caspian Sea regions), *B. balearica* (Mediterranean basin), *B. bodinieri* (China), *B. glomerata* (Cuba and Hispaniola), *B. harlandii* (China to Vietnam), *B. macowanii* (South Africa), *B. riparia* (Japan), *B. wallichiana* (Himalayas from east Afghanistan to Nepal), at least three *Pachysandra* species including the endangered *P. procumbens* (eastern United States), and several *Sarcococca* species (East Asia). More studies on the susceptibility of Buxaceae species to infection are needed to better assess the risk of the pathogen establishing and causing ecological harm.

Our global climatic suitability models for *Cps* provide some of the first insights into the potential geographic origin of the pathogen, which is still unknown (Castroagudín et al. 2020a, LeBlanc et al. 2021). The CLIMEX and ensemble correlative model both included a large part of southeastern China and Japan in the potential distribution, a finding which supports the hypothesis that the pathogen may have arrived to Europe on boxwood plants from East Asia (Daughtrey 2019). A possible origin of *Cps* from China is consistent with reports that most non-European imports of *Buxus* species to Europe come from this country (EPPO 2012), and with a leading hypothesis for the likely origin of invasive box tree moth in Europe (Van der Straten and

683 Muus 2010, CABI 2021). Nonetheless, we cannot rule out the possibility that *Cps* is native to
684 another host center of diversity for *Buxus* or other Buxaceae species such as in the Caribbean or
685 Madagascar (Castroagudín et al. 2020a), particularly given that at least one of the modeling
686 approaches included parts of these regions in the potential distribution.
687
688 *Model uncertainty*
689 Discordance between CLIMEX and ensemble correlative model predictions for *Cps* in
690 Europe, western Asia, and North America primarily occurred at the predicted range edges. The
691 potential distribution according to the ensemble correlative model extended somewhat farther
692 north in Europe and the eastern United States, and farther east in the southeastern United States.
693 Conversely, the potential distribution according to CLIMEX extended slightly farther east in
694 Europe and included the border region of Russia. However, ensemble correlative model
695 predictions for areas of discordance with CLIMEX should be interpreted with caution because
696 predictions also varied among the six different correlative models, which indicates uncertainty
697 both across and within modeling approaches (i.e. process-based vs. correlative models and
698 correlative vs. correlative models). These findings are consistent with studies showing that model
699 type is a primary source of uncertainty when predicting species distributions, and that uncertainty
700 is often greater at range margins compared with range cores (Marmion et al. 2009, Capinha and
701 Anastácio 2011, Vale et al. 2014, Watling et al. 2015, Shabani et al. 2016).
702 Global projections of the ensemble correlative model were particularly discordant with
703 the CLIMEX model for equatorial regions. We focused more on interpreting CLIMEX model
704 predictions for equatorial regions because the MOP analysis indicated that dissimilarity in
705 climate for the calibration and projection area was highest for equatorial areas, which suggests
706 that predictions there may be unreliable (Zurell et al. 2012, Owens et al. 2013, Higgins et al.
707 2020). Process-based models such as CLIMEX are thought to be more reliable in predicting a
708 species' potential distribution in novel climates than correlative models because they rely on
709 proximate constraints limiting distributions, rather than on model extrapolations (Kearney and
710 Porter 2009, Evans et al. 2016, Higgins et al. 2020). For example, most equatorial areas that were
711 included in the potential distribution by the ensemble correlative model were predicted to be
712 excluded by heat stress in the CLIMEX model, including those in central Africa, India, and
713 mainland Southeast Asia (Indochina and Malay peninsulas). Heat stress is measured using

thresholds and rates that were calibrated using ecophysiological information and records for the pathogen in the hottest parts of its known distribution, and its predicted role in shaping the potential distribution of *Cps* seems realistic given present-day knowledge of the species. As the occurrence record dataset for model fitting influences projections into new areas, future work should investigate whether *Cps* has persisted at localities used to fit correlative models for this study (Appendix S1, Supporting information), particularly in newly invaded areas such as those in the southern, midwestern, and Pacific coast region of North America. Records from newly invaded areas could potentially represent short-term establishments, such as during a year(s) with favorable weather, and may therefore be excluded from future presence-only correlative modeling analyses.

Future climate-based risk mapping studies for *Cps* which use more recent climate data and potentially incorporate inter-annual variability into models may provide more robust estimates of present-day risk. Our models used historical 30-year climate normals for 1961 to 1990 because the current version of CLIMEX has no native ability to import and process other forms of gridded data, such as climate normals for a more recent time frame (e.g., 1991–2021). Additionally, CliMond data for more recent time frames have not been developed to our knowledge, which hinders making a comparison of correlative models based on the same set of climate predictors for different time frames. Global temperatures and precipitation patterns have significantly changed even over the past 30 years (USGCRP 2018, IPCC 2021), which suggests that climatic suitability models for *Cps* could misrepresent establishment risk in areas where climates have become more (or less) favorable for the pathogen's growth and survival. For example, higher minimum winter temperatures or decreased frequency or intensity of extreme cold resulting from climate change may increase rates of overwintering survival for invasive microbial pathogens (Dukes et al. 2009, Thakur et al. 2019), which raises the possibility that establishment risk at the northernmost range edges of *Cps* may be higher than our models predict. Additionally, increasing humidity, precipitation, and rising temperatures in certain regions such as the midwestern United States (USGCRP 2018, IPCC 2021) could increase risk of establishment, whereas aridification in regions such as southern Europe, western and central Asia, and western North America (IPCC 2021) may reduce risk. Climate suitability models which account for inter-annual variations may increase the accuracy of predictions for *Cps* under climate change because biologically relevant climatic variation that can arise from events such as

droughts or heat waves may be obscured in aggregated climate datasets such as 30-year climate normals (Gardner et al. 2021).

Conclusions

In developing species distribution models for *Cps* and evaluating the role of climatic factors in shaping its known range limits, we have provided some of the first insights into the potential invasive distribution and geographic origin of the most widespread and damaging pathogens of boxwood. Understanding where the pathogen could establish is particularly important in light of evidence for intercontinental dispersal and multiple introductions of *Cps* in the United States, which suggests that introductions of the pathogen are common and will likely continue to occur (Castroagudín et al. 2020a, LeBlanc et al. 2021). The CLIMEX and ensemble correlative model are consistent in predicting the potential for further spread in Europe (southern and eastern Europe), and in North America (southern, midwestern, and Pacific coast region). While our models can assist with identifying areas to watch for *Cps* both regionally and globally, an assessment of local climates for a target area may provide greater insight into the likelihood of the establishment. For example, the pathogen's limited presence in areas of the potential distribution in Europe and North America which have Mediterranean and humid continental climates may suggest that regions of the global potential distribution with similar climates are at lower risk of establishment. Locations which are climatically marginal for *Cps*, but which have extensive boxwood plantings, may be best able to exclude or eradicate boxwood blight outbreaks by implementing best practices such as using less dense plantings, limiting shade cover, and exclusively make use of underground irrigation (Bush et al. 2016, Dart et al. 2016, Daughtrey 2019). Additionally, the avoidance of highly susceptible cultivars including *Buxus sempervirens* 'Suffruticosa' and *Buxus sempervirens* (Shishkoff et al. 2015; LaMondia and Shishkoff 2017; LeBlanc et al. 2018; Kramer et al. 2020) may help reduce the risk of establishment. Surveillance of *Cps* in regions of the world that fall within the potential distribution of the pathogen and have native Buxaceae species will be key for early detection and rapid responses measures.

Future modeling work that uses current climate data to evaluate risk of establishment may provide better insights into potential range limits for *Cps*, such as in high-elevation or high-latitude areas where the pathogen may now be capable of survival due to warming temperatures in recent decades. The CLIMEX model developed for this study could be modified to predict the

776 potential distribution of *C. henricotiae*, a closely related but genetically distinct species that also
777 causes boxwood blight (Gehesquière et al. 2016, LeBlanc et al. 2021). To date *C. henricotiae* has
778 only been found in five countries in Europe, but further range expansion of this pathogen is
779 expected and would likely influence boxwood blight epidemiology in the landscape because its
780 thermotolerance is greater than *Cps* (Miller et al. 2018, LeBlanc et al. 2021).
781
782
783 **Data availability**
784 The data, metadata, code, and derived products to reproduce the analysis and figures have been
785 archived at Zenodo (https://doi.org/XX.XXXX/zenodo.XXXXXXX).
786
787 **Funding**
788 This work was funded by USDA APHIS Cooperative Agreement No. 20-8130-0282-CA.
789
790 **Competing interests**
791 The authors have declared that no competing interests exist.
792
793 **Acknowledgements**
794 We extend our thanks to Thomas Brand, Manus Gammelgard, Iryna Matsiakh, Nicole Ward-
795 Gauthier, Fulya Baysal-Gurel, Funda Oskay, and Jerry Weiland for providing geographic
796 location information for *Cps* occurrence records.

References

Aiello-Lammens ME, Boria RA, Radosavljevic A, Vilela B, Anderson R. (2015) spThin: an R package for spatial thinning of species occurrence records for use in ecological niche models. Ecography 38: 541–545. https://doi.org/https://doi.org/10.1111/ecog.01132

Akili S, Katircioglu YZ, Zor K, Maden S (2012) First report of blight on *Buxus* spp. caused by *Cylindrocladium pseudonaviculatum* in the Eastern Black Sea region of Turkey. Plant Disease 87: 1539. https://doi.org/10.1094/PDIS.2003.87.12.1539A

Allouche O, Tsoar A, Kadmon R (2006) Assessing the accuracy of species distribution models: prevalence, kappa and the true skill statistic (TSS). Journal of Applied Ecology 43: 1223–1232. https://doi.org/10.1111/j.1365-2664.2006.01214.x

de Andrade AFA, Velazco SJE, De Marco Júnior P (2020) ENMTML: An R package for a straightforward construction of complex ecological niche models. Environmental Modelling and Software 125: 104615. https://doi.org/10.1016/j.envsoft.2019.104615

Anonymous (2012) New plant disease - boxwood blight. Tillamook County Tiller: 1.

Avenot HF, King C, Edwards TP, Baudoin A, Hong CX (2017) Effects of inoculum dose, temperature, cultivar, and interrupted leaf wetness period on infection of boxwood by *Calonectria pseudonaviculata*. Plant Disease 101: 866–873. https://doi.org/10.1094/pdis-05-16-0742-re

Balthazar M von, Endress PK, Qiu YL (2000) Phylogenetic relationships in Buxaceae based on nuclear internal transcribed spacers and plastid ndhF sequences. International Journal of Plant Sciences 161: 785–792. https://doi.org/10.1086/314302

Bartíková M, Holková L, Šafránková I (2020a) Occurrence of boxwood blight (*Calonectria pseudonaviculata* and *C. henricotiae*) in historical gardens in the Czech Republic. European Journal of Plant Pathology 158: 135–142. https://doi.org/10.1007/s10658-020-02061-2

Bartíková M, Brand T, Beltz H, Šafránková I (2020b) Host susceptibility and microclimatic conditions influencing the development of blight diseases caused by *Calonectria henricotiae*. European Journal of Plant Pathology 157: 103–117. https://doi.org/10.1007/s10658-020-01986-y

Batdorf L (2005) Boxwood Handbook—A Practical Guide to Knowing and Growing Boxwood. 3rd ed. The American Boxwood Society, Boyces, Virginia, USA, 123 pp.

Beaumont L, Gallagher R, Thuiller W, Downey P, Leishman M, Hughes L (2009) Different

climatic envelopes among invasive populations may lead to underestimations of current and future biological invasions. Diversity and Distributions 15: 409–420. https://doi.org/10.1111/j.1472-4642.2008.00547.x

Blomquist CL, Kosta KL, Santos PF, Rooney-Latham S (2018) First report of boxwood blight caused by *Calonectria pseudonaviculata* in California. Plant Disease 102: 2379–2379. https://doi.org/https://doi.org/10.1094/PDIS-05-18-0765-PDN

Boyce MS, Vernier PR, Nielsen SE, Schmiegelow FKA (2002) Evaluating resource selection functions. Ecological Modelling 157: 281–300. https://doi.org/https://doi.org/10.1016/S0304-3800(02)00200-4

Bush E, Hansen MA, Dart N, Hong C, Bordas A, Likins TM (2016) Best management practices for boxwood blight in the Virginia home landscape. Virginia Cooperative Extension Publication PPWS-85NP. Virginia Tech, VA. Online: https://vtechworks.lib.vt.edu/bitstream/handle/10919/80658/PPWS-29.pdf.

CABI (2021) *Cydalima perspectalis* (box tree moth). Invasive Species Copendium. Wallingford, UK: CAB International. www.cabi.org/isc.

Capinha C, Anastácio P (2011) Assessing the environmental requirements of invaders using ensembles of distribution models. Diversity and Distributions 17: 13–24. https://doi.org/10.1111/j.1472-4642.2010.00727.x

Castroagudín VL, Weiland JE, Baysal-Gurel F, Cubeta MA, Daughtrey ML, Gauthier NW, LaMondia J, Luster DG, Hand FP, Shishkoff N, Williams-Woodward J, Yang X, LeBlanc N, Crouch JA (2020a) One clonal lineage of *Calonectria pseudonaviculata* is primarily responsible for the boxwood blight epidemic in the United States. Phytopathology 110: 1845–1853. https://doi.org/10.1094/PHYTO-04-20-0130-R

Castroagudín VL, Yang X, Daughtrey ML, Luster DG, Pscheidt JW, Weiland JE, Crouch JA (2020b) Boxwood blight disease: A diagnostic guide. Plant Health Progress 21: 291–300. https://doi.org/10.1094/PHP-06-20-0053-DG

Caudullo G, Welk E, San-Miguel-Ayanz J (2017) Chorological maps for the main European woody species. Data in Brief 12: 662–666. https://doi.org/10.1016/j.dib.2017.05.007

Cech T, Diminic D, Heungens K (2010) *Cylindrocladium buxicola* causes common box blight in Croatia. Plant Pathology 59: 1169–1169. https://doi.org/10.1111/j.1365-3059.2010.02332.x

Cobos ME, Townsend Peterson A, Barve N, Osorio-Olvera L (2019) kuenm: an R package for

detailed development of ecological niche models using Maxent. PeerJ 7: e6281. https://doi.org/10.7717/peerj.6281

Cooper JC, Soberón J (2018) Creating individual accessible area hypotheses improves stacked species distribution model performance. Global Ecology and Biogeography 27: 156–165. https://doi.org/10.1111/geb.12678

Crous PW, Groenewald JZ, Hill CF (2002) *Cylindrocladium pseudonaviculatum* sp. nov. from New Zealand, and new *Cylindrocladium* records from Vietnam. Sydowia 54: 23–34.

Dart N, Hong C, Craig CA, Fry JT, Hu X (2015) Soil inoculum production, survival, and infectivity of the boxwood blight pathogen, *Calonectria pseudonaviculata*. Plant Disease 99: 1689–1694. https://doi.org/10.1094/PDIS-12-14-1245-RE

Dart N, Hong C, Bordas A, Bush E, Hansen M, Likins T (2016) Best management practices for boxwood blight in Virginia retail nurseries WITHOUT boxwood blight. Virginia Cooperative Extension Publication No. PPWS-35NP. Available at: http://pubs.ext.vt.edu/PPWS/PPWS-35/PPWS-35.html.

Daughtrey ML (2019) Boxwood blight: threat to ornamentals. Annual Review of Phytopathology 57: 189–209. https://doi.org/10.1146/annurev-phyto-082718-100156

Di Domenico F, Lucchese F, Magri D (2012) *Buxus* in Europe: Late Quaternary dynamics and modern vulnerability. Perspectives in Plant Ecology, Evolution and Systematics 14: 354–362. https://doi.org/10.1016/j.ppees.2012.07.001

Dormann CF, Schymanski SJ, Cabral J, Chuine I, Graham C, Hartig F, Kearney MR, Morin X, Römermann C, Schröder B, Singer A (2012) Correlation and process in species distribution models: Bridging a dichotomy. Journal of Biogeography 39: 2119–2131. https://doi.org/10.1111/j.1365-2699.2011.02659.x

Dormann CF, Elith J, Bacher S, Buchmann C, Carl G, Carré G, Marquéz JRG, Gruber B, Lafourcade B, Leitão PJ, Münkemüller T, McClean C, Osborne PE, Reineking B, Schröder B, Skidmore AK, Zurell D, Lautenbach S (2013) Collinearity: a review of methods to deal with it and a simulation study evaluating their performance. Ecography 36: 027–046. https://doi.org/10.1111/j.1600-0587.2012.07348.x

Douglas SM (2012) Boxwood blight — a new threat to boxwood in the U.S. CNLA/CGGA Winter Symposium, Plantsville, CT. Available at: https://nationalplantboard.org/wp-content/uploads/docs/2012_meeting/npb_2012_bwb.pdf (Accessed July 27, 2021).

890 Dukes JS, Jennifer Pontius, David Orwig, Jeffrey RG, Vikki LR, Nicholas Brazee, Barry Cooke,
891 Kathleen AT, Erik ES, Robin Harrington, Joan Ehrenfeld, Jessica Gurevitch, Manuel
892 Lerdau, Kristina Stinson, Robert Wick, Matthew Ayres (2009) Responses of insect pests,
893 pathogens, and invasive plant species to climate change in the forests of northeastern North
894 America: What can we predict? Canadian Journal of Forest Research 39: 231–248.
895 https://doi.org/10.1139/X08-171
896 Elith J, Graham CH (2009) Do they? How do they? WHY do they differ? On finding reasons for
897 differing performances of species distribution models. Ecography 32: 66–77.
898 https://doi.org/10.1111/j.1600-0587.2008.05505.x
899 Elith J, Leathwick JR, Hastie T (2008) A working guide to boosted regression trees. The Journal
900 of animal ecology 77: 802–13. https://doi.org/10.1111/j.1365-2656.2008.01390.x
901 Elmhirst JF, Auxier BE, Wegener LA (2013) First report of box blight caused by
902 *Cylindrocladium pseudonaviculatum* in British Columbia, Canada. Plant Disease 97: 559.
903 https://doi.org/https://doi.org/10.1094/PDIS-10-12-0927-PDN
904 EPPO (2012) EPPO study on the risk of imports of plants for planting, 1061. Paris, France:
905 European and Mediterranean Plant Protection Organization, 75 pp.
906 www.eppo.int/QUARANTINE/EPPO_Study_on_Plants_for_planting.pdf.
907 EPPO (2020) *Calonectria pseudonaviculata* (CYLDBU). Available at:
908 http://https://gd.eppo.int/taxon/CYLDBU/distribution (Accessed 2021 May 5).
909 Evans J. (2021) spatialEco. R package Version 1.3-6. https://github.com/jeffreyevans/spatialEco.
910 Evans MEK, Merow C, Record S, McMahon SM, Enquist BJ (2016) Towards process-based
911 range modeling of many species. Trends in Ecology and Evolution 31: 860–871.
912 https://doi.org/10.1016/j.tree.2016.08.005
913 Fisher MC, Henk DA, Briggs CJ, Brownstein JS, Madoff LC, McCraw SL, Gurr SJ (2012)
914 Emerging fungal threats to animal, plant and ecosystem health. Nature 484: 186–194.
915 https://doi.org/10.1038/nature10947
916 França S, Cabral HN (2019) Distribution models of estuarine fish species: the effect of sampling
917 bias, species ecology and threshold selection on models' accuracy. Ecological Informatics
918 51: 168–176. https://doi.org/10.1016/j.ecoinf.2019.03.005
919 Friss I (1989) A synopsis of the Buxaceae in Africa south of the Sahara. Kew Bulletin 44: 293–
920 299.

921 Gardner AS, Gaston KJ, Maclean IMD (2021) Accounting for inter-annual variability alters
922 long-term estimates of climate suitability. Journal of Biogeography 48: 1960–1971.
923 https://doi.org/10.1111/jbi.14125
924 Gasich EL, Kazartsev IA, Gannibal PB, Koval AG, Shipilova NP, Khlopunova LB,
925 Ovsyannikova EI (2013) *Calonectria pseudonaviculata* - a new for Abkhazia species, the
926 causal agent of boxwood blight. Mikologiya I Fitopatologiya 47: 129–131.
927 Gehesquière B (2014) *Cylindrocladium buxicola* nom. cons. prop. (syn. Calonectria
928 pseudonaviculata) on *Buxus:* molecular characterization, epidemiology, host resistance and
929 fungicide control. PHD Thesis. Ghent University (Ghent, Belgium)
930 Gehesquière B, D'Haeyer S, Pham KTK, Van Kuik AJ, Maes M, Höfte M, Heungens K (2013)
931 qPCR assays for the detection of *Cylindrocladium buxicola* in plant, water, and air samples.
932 Plant Disease 97: 1082–1090. https://doi.org/10.1094/PDIS-10-12-0964-RE
933 Gehesquière B, Crouch JA, Marra RE, Van Poucke K, Rys F, Maes M, Gobin B, Höfte M,
934 Heungens K (2016) Characterization and taxonomic reassessment of the box blight
935 pathogen *Calonectria pseudonaviculata*, introducing Calonectria henricotiae sp. nov. Plant
936 Pathology 65: 37–52. https://doi.org/10.1111/ppa.12401
937 Golding N, Purse BV (2016) Fast and flexible Bayesian species distribution modelling using
938 Gaussian processes. Methods in Ecology and Evolution 7: 598–608.
939 https://doi.org/10.1111/2041-210X.12523
940 Gorgiladze L, Meparishvili G, Sikharulidze Z, Natsarishvili K, Davitadze R (2011) First report
941 of *Cylindrocladium buxicola* in Georgia. Plant Disease 23: 24.
942 https://doi.org/10.1094/PDIS-93-6-0670B
943 Guisan A, Edwards TC, Hastie T (2002) Generalized linear and generalized additive models in
944 studies of species distributions: setting the scene. Ecological Modelling 157: 89–100.
945 https://doi.org/https://doi.org/10.1016/S0304-3800(02)00204-1
946 Guo Q, Kelly M, Graham CH (2005) Support vector machines for predicting distribution of
947 Sudden Oak Death in California. Ecological Modelling 182: 75–90.
948 https://doi.org/10.1016/j.ecolmodel.2004.07.012
949 Gutiérrez PAG (2014) Evolution and biogeography of *Buxus* L. (Buxaceae) in Cuba and the
950 Caribbean. PHD Thesis. Free University of Berlin (Berlin, Germany)
951 Hall C (2021) Observations regarding the value of boxwood sales from 2014 to 2019. Boxwood

Blight Insight Group Newsletter 2: 1–2.

Hall CR, Hong C, Gouker FE, Daughtrey M (2021) Analyzing the structural shifts in U.S. boxwood production due to boxwood blight. Journal of Environmental Horticulture 39: 91–99. https://doi.org/10.24266/0738-2898-39.3.91

Hao T, Elith J, Lahoz-Monfort JJ, Guillera-Arroita G (2020) Testing whether ensemble modelling is advantageous for maximising predictive performance of species distribution models. Ecography 43: 549–558. https://doi.org/10.1111/ecog.04890

Henricot B (2006) Box blight rampages onwards. The Plantsman: 153–157.

Henricot B, Pérez Sierra A, Prior C (2000) A new blight disease on *Buxus* in the UK caused by the fungus *Cylindrocladium*. Plant Pathology 49: 805. https://doi.org/10.1046/j.1365-3059.2000.00508.x

Henricot B, Gorton C, Denton G, Denton J (2008) Studies on the control of *Cylindrocladium buxicola* using fungicides and host resistance. Plant Disease 92: 1273–1279. https://doi.org/10.1094/PDIS-92-9-1273

Henricot BB, Culham A (2002) *Cylindrocladium buxicola*, a new species affecting *Buxus* spp., and its phylogenetic status. Mycologia 94: 980. https://doi.org/10.1080/15572536.2003.11833155

Higgins SI, Larcombe MJ, Beeton NJ, Conradi T, Nottebrock H (2020) Predictive ability of a process-based versus a correlative species distribution model. Ecology and Evolution 10: 11043–11054. https://doi.org/10.1002/ece3.6712

Hijmans RJ, Cameron SE, Parra JL, Jones PG, Jarvis A (2005) Very high resolution interpolated climate surfaces for global land areas. International Journal of Climatology 25: 1965–1978. https://doi.org/10.1002/joc.1276

Hong C (2019a) Fighting pathogens together. Science 365: 229. https://doi.org/10.1126/science.aay4514

Hong C (2019b) Saving American gardens from boxwood blight. The Boxwood Bulletin 58: 3–10.

Hūšang A (1989) Boxtree. Encyclopedia Iranica, Vol. IV, pp. 418-420; available at: https://iranicaonline.org/articles/boxtree-buxus-l (accessed 23 June 2021). Encyclopedia Iranica, Vol. IV 4: 418–420.

IPCC (2021) Climate Change 2021: The Physical Science Basis. Contribution of Working Group

I to the Sixth Assessment Report of the Intergovernmental Panel on Climate Change. Masson-Delmotte V, Zhai P, Pirani A, Connors SL, Péan C, Berger S, Caud N, Chen Y, Goldfarb L, Gomis MI, Huang M, Leitzell K, Lonnoy E, Matthews JBR, Maycock TK, Waterfield T, O.Yelekçi, Yu R, Zhou B (Eds). Cambridge University Press, Cambridge, U.K.

Ireland KB, Kriticos DJ (2019) Why are plant pathogens under-represented in eco-climatic niche modelling? International Journal of Pest Management 65: 207–216. https://doi.org/10.1080/09670874.2018.1543910

Iriarte F, Paret M, Knox G, Schubert T, Jeyaprakash A, Davison D (2016) First report of boxwood blight caused by *Calonectria pseudonaviculata* in Florida. Plant Health Progress 17: 229–231. https://doi.org/10.1094/PHP-BR-16-0027

Ivors KL, Lacey LW, Milks DC, Douglas SM, Inman MK, Marra RE, LaMondia JA (2012) First report of boxwood blight caused by *Cylindrocladium pseudonaviculatum* in the United States. Plant Disease 96: 1070–1070. https://doi.org/10.1094/PDIS-03-12-0247-PDN

Kearney MR, Porter W (2009) Mechanistic niche modelling: Combining physiological and spatial data to predict species' ranges. Ecology Letters 12: 334–350. https://doi.org/10.1111/j.1461-0248.2008.01277.x

Khazaeli P, Rezaee S, Mirabolfathy M, Zamanizadeh H, Kia-daliri SK (2015) Report of boxwood blight extension to Golestan province forests. Applied Entomology and Phytopathology 83: 85–86.

Khazaeli P, Rezaee S, Mirabolfathy M, Zamanizade H, Kiadaliri H (2018) Genetic and phenotypic variation of *Calonectria pseudonaviculata* isolates causing boxwood blight disease in the Hyrcanian forest of Iran. Agricultural Research & Technology: Open Access Journal 19: 556081. https://doi.org/10.19080/artoaj.2018.19.556081

Köhler E (2014) Buxaceae. In: Greute W, Rankin-Rodríguez R (Eds), Flora de la República de Cuba. Fasciculo 19(1). Koeltz Scientific Books, Oberreifenberg, Germany, 1–124.

Köhler E, Brückner P (1989) The genus *Buxus* (Buxaceae): aspects of its differentiation in space and time. Plant Systematics and Evolution 162: 267–283.

Kolganikhina GB (2014) Year dynamics of the Colchis box health status and *Cylindrocladium* box blight development in the Sochi national park. Russian Journal of Ecology 6: 202–209.

Kong P, Hong C (2019) Host responses and impact on the boxwood blight pathogen, *Calonectria*

pseudonaviculata. Planta 249: 831–838. https://doi.org/10.1007/s00425-018-3041-4

Kong P, Likins TM, Hong CX (2017) First report of *Pachysandra terminalis* leaf spot by Calonectria pseudonaviculata in Virginia. Plant Disease 101: 509–509. https://doi.org/https://doi.org/10.1094/PDIS-10-16-1513-PDN

Kramer-Schadt S, Niedballa J, Pilgrim JD, Schröder B, Lindenborn J, Reinfelder V, Stillfried M, Heckmann I, Scharf AK, Augeri DM, Cheyne SM, Hearn AJ, Ross J, Macdonald DW, Mathai J, Eaton J, Marshall AJ, Semiadi G, Rustam R, Bernard H, Alfred R, Samejima H, Duckworth JW, Breitenmoser-Wuersten C, Belant JL, Hofer H, Wilting A (2013) The importance of correcting for sampling bias in MaxEnt species distribution models. Diversity and Distributions 19: 1366–1379. https://doi.org/10.1111/ddi.12096

Kriticos DJ, Maywald GF, Yonow T, Zurcher EJ, Herrmann N, Sutherst RW (2016) CLIMEX Version 4: Exploring the effects of climate on plants, animals and diseases. In: CSIRO, Canberra, Australia. Available at: https://www.hearne.software/getattachment/199e1f3e-460a-4ac8-8f7f-1eeee84110c7/Climex-v4-User-Guide.aspx.

Kriticos DJ, Webber BL, Leriche A, Ota N, Macadam I, Bathols J, Scott JK (2012) CliMond: global high-resolution historical and future scenario climate surfaces for bioclimatic modelling. Methods in Ecology and Evolution 3: 53–64. https://doi.org/10.1111/j.2041-210X.2011.00134.x

LaMondia JA (2015) Management of *Calonectria pseudonaviculata* in boxwood with fungicides and less susceptible host species and varieties. Plant Disease 99: 363–369. https://doi.org/10.1094/PDIS-02-14-0217-RE

LaMondia JA, Li DW (2013) *Calonectria pseudonaviculata* can cause leaf spot and stem blight of *Pachysandra procumbens*. Plant Health Progress 14: Online. https://doi.org/https://doi.org/10.1094/PHP-2013-0226-01-BR

LaMondia JA, Shishkoff N (2017) Susceptibility of boxwood accessions from the national boxwood collection to boxwood blight and potential for differences between *Calonectria pseudonaviculata* and *C. henricotiae*. HortScience 52: 873–879. https://doi.org/10.21273/HORTSCI11756-17

LaMondia JA, Li DW, Marra RE, Douglas SM (2012) First report of *Cylindrocladium pseudonaviculatum* causing leaf spot of Pachysandra terminalis. Plant Disease 96: 1069. https://doi.org/10.1094/PDIS-03-12-0235-PDN

1045 Lantschner MV, de la Vega G, Corley JC (2019) Predicting the distribution of harmful species
1046 and their natural enemies in agricultural, livestock and forestry systems: an overview.
1047 International Journal of Pest Management 65: 190–206.
1048 https://doi.org/10.1080/09670874.2018.1533664
1049 LeBlanc N, Salgado-Salazar C, Crouch JA (2018) Boxwood blight: an ongoing threat to
1050 ornamental and native boxwood. Applied Microbiology and Biotechnology 102: 4371–
1051 4380. https://doi.org/10.1007/s00253-018-8936-2
1052 LeBlanc N, Cubeta MA, Crouch JA (2021) Population genomics trace clonal diversification and
1053 intercontinental migration of an emerging fungal pathogen of boxwood. Phytopathology
1054 111: 184–193. https://doi.org/10.1094/PHYTO-06-20-0219-FI
1055 Lehtijärvi A, Doğmuş-Lehtijärvi HT, Oskay F (2017) Boxwood blight in Turkey: impact on
1056 natural boxwood populations and management challenges. Baltic Forestry 23: 274–278.
1057 Leroy B, Delsol R, Hugueny B, Meynard CN, Barhoumi C, Barbet-Massin M, Bellard C (2018)
1058 Without quality presence–absence data, discrimination metrics such as TSS can be
1059 misleading measures of model performance. Journal of Biogeography 45: 1994–2002.
1060 https://doi.org/10.1111/jbi.13402
1061 Leutner B, Horning N (2017) Rstoolbox: tools for remote sensing data analysis. R Package
1062 Version 0.2.6. Available online: https://cran.r-
1063 project.org/web/packages/RStoolbox/index.html.
1064 Li W, Guo Q (2013) How to assess the prediction accuracy of species presence-absence models
1065 without absence data? Ecography 36: 788–799. https://doi.org/10.1111/j.1600-
1066 0587.2013.07585.x
1067 Liu C, Berry PM, Dawson TP, Pearson RG (2005) Selecting thresholds of occurrence in the
1068 prediction of species distributions. Ecography 28: 385–393. https://doi.org/10.1111/j.0906-
1069 7590.2005.03957.x
1070 Lombard L, Crous PW, Wingfield BD, Wingfield MJ (2010) Systematics of *Calonectria*: a
1071 genus of root, shoot and foliar pathogens. Studies in Mycology 66: 1–71.
1072 https://doi.org/10.1016/s0166-0616(14)60020-8
1073 Lovett GM, Weiss M, Liebhold AM, Holmes TP, Leung B, Lambert KF, Orwig DA, Campbell
1074 FT, Rosenthal J, McCullough DG, Wildova R, Ayres MP, Canham CD, Foster DR, LaDeau
1075 SL, Weldy T (2016) Nonnative forest insects and pathogens in the United States: Impacts

and policy options. Ecological Applications 26: 1437–1455. https://doi.org/10.1890/15-1176

Magarey RD, Fowler GA, Borchert DM, Sutton TB, Colunga-Garcia M, Simpson JA, Health P, Service I, Colunga-Garcia M (2007) NAPPFAST: an internet system for the weather-based mapping of plant pathogens. Plant Disease 91: 336–345. https://doi.org/10.1094/PDIS-91-4-0336

Malapi-Wight M, Salgado-Salazar C, Demers JE, Clement DL, Rane KK, Crouch JA (2016) Sarcococca blight: Use of whole-genome sequencing for fungal plant disease diagnosis. Plant Disease 100: 1093–1100. https://doi.org/10.1094/PDIS-10-15-1159-RE

De Marco P, Nóbrega CC (2018) Evaluating collinearity effects on species distribution models: An approach based on virtual species simulation. PLoS ONE 13: e0202403. https://doi.org/10.1371/journal.pone.0202403

Marmion M, Parviainen M, Luoto M, Heikkinen RK, Thuiller W (2009) Evaluation of consensus methods in predictive species distribution modelling. Diversity and Distributions 15: 59–69. https://doi.org/10.1111/j.1472-4642.2008.00491.x

Matsiakh I (2016) Assessment of forest pests and diseases in native boxwood forests of Georgia: Final report. In: Forestry Department, Ukrainian National Forestry University (Lviv). Available at: https://www.enpi-fleg.org/site/assets/files/1939/assessment_of_pests_and_diseases_in_georgian_forests_i_matsiakh_final_final.pdf. Available from: https://www.enpi-fleg.org/site/assets/files/1939/assessment_of_pests_and_diseases_in_georgian_forests_i_matsiakh_final_final.pdf.

Matsiakh I, Kramarets V, Mamadashvili G (2018) Box tree moth *Cydalima perspectalis* as a threat to the native populations of *Buxus colchica* in Republic of Georgia. Journal of the Entomological Research Society 20: 29–42.

Miller ME, Shishkoff N, Cubeta MA (2018) Thermal sensitivity of *Calonectria henricotiae* and Calonectria pseudonaviculata conidia and microsclerotia. Mycologia 110: 546–558. https://doi.org/10.1080/00275514.2018.1465778

Mirabolfathy M (2013) Outbreak of boxwood tree leaf drop in Guilan and Mazandaran forests. In: 1st Iranian Mycological Congress. University of Guilan, Rasht, Iran, 8.

Mirabolfathy M, Ahangaran Y, Lombard L, Crous PW (2013) Leaf blight of *Buxus sempervirens*

in northern forests of Iran caused by *Calonectria pseudonaviculata*. Plant Disease 97: 1121. https://doi.org/10.1094/PDIS-03-13-0237-PDN

Mitchell R, Chitanava S, Dbar R, Kramarets V, Lehtijärvi A, Matchutadze I, Mamadashvili G, Matsiakh I, Nacambo S, Papazova-Anakieva I, Sathyapala S, Tuniyev B, Vétek G, Zukhbaia M, Kenis M (2018) Identifying the ecological and societal consequences of a decline in *Buxus* forests in Europe and the Caucasus. Biological Invasions 20: 3605–3620. https://doi.org/10.1007/s10530-018-1799-8

Nahrung HF, Carnegie AJ (2020) Non-native forest insects and pathogens in Australia: establishment, spread, and impact. Frontiers in Forests and Global Change 3: 1–12. https://doi.org/10.3389/ffgc.2020.00037

Owens HL, Campbell LP, Dornak LL, Saupe EE, Barve N, Soberón J, Ingenloff K, Lira-Noriega A, Hensz CM, Myers CE, Peterson AT (2013) Constraints on interpretation of ecological niche models by limited environmental ranges on calibration areas. Ecological Modelling 263: 10–18. https://doi.org/10.1016/j.ecolmodel.2013.04.011

Paini DR, Sheppard AW, Cook DC, Barro PJ De, Worner SP, Thomas MB (2016) Global threat to agriculture from invasive species. Proceedings of the National Academy of Sciences 113: 7575–7579. https://doi.org/10.1073/pnas.1602205113

Palmer CL, Shishkoff N (2014) Boxwood blight: a new scourge, a new paradigm for collaborative research. Outlooks on Pest Management 25: 230–236. https://doi.org/10.1564/v25_jun_10

Panahi P, Jamzad Z, Jalili A, Sagheb Talebi K, Pourhashemi M (2021) The role of the National Botanical Garden of Iran in ex situ conservation of *Buxus hyrcana* Pojark.; An endangered species. Urban Forestry & Urban Greening 57: 126951. https://doi.org/10.1016/j.ufug.2020.126951

Patarkalashvili T (2017) Forest biodiversity of Georgia and endangered plant species. Annals of Agrarian Science 15: 349–351. https://doi.org/10.1016/j.aasci.2017.06.002

Peterson AT, Papeş M, Soberón J (2015) Mechanistic and correlative models of ecological niches. European Journal of Ecology 1: 28–38. https://doi.org/10.1515/eje-2015-0014

Petitpierre B, Broennimann O, Kueffer C, Daehler C, Guisan A (2017) Selecting predictors to maximize the transferability of species distribution models: lessons from cross-continental plant invasions. Global Ecology and Biogeography 26: 275–287.

https://doi.org/10.1111/geb.12530

Pfender WF, Gent DH, Mahaffee WF (2012) Sensitivity of disease management decision aids to temperature input errors associated with sampling interval and out-of-canopy sensor placement. Plant Disease 96: 726–736. https://doi.org/10.1094/PDIS-03-11-0262

Phillips SJ, Anderson RP, Schapire RE (2006) Maximum entropy modeling of species geographic distributions. Ecological Modelling 190: 231–259. https://doi.org/10.1016/j.ecolmodel.2005.03.026

Phillips SJ, Anderson RP, Dudík M, Schapire RE, Blair ME (2017) Opening the black box: an open-source release of Maxent. Ecography 40: 887–893. https://doi.org/10.1111/ecog.03049

Pili AN, Tingley R, Sy EY, Diesmos MLL, Diesmos AC (2020) Niche shifts and environmental non-equilibrium undermine the usefulness of ecological niche models for invasion risk assessments. Scientific Reports 10: 1–18. https://doi.org/10.1038/s41598-020-64568-2

Pintos Varela C, Penalta BG, Vázquez JPM, Casal OA (2009) First report of *Cylindrocladium buxicola* on *Buxus sempervirens* in Spain. Plant Disease 93: 670–670. https://doi.org/https://doi.org/10.1094/PDIS-93-6-0670B

Prasad AM, Iverson LR, Liaw A (2006) Newer classification and regression tree techniques: bagging and random forests for ecological prediction. Ecosystems 9: 181–199. https://doi.org/10.1007/s10021-005-0054-1

R Development Core Team (2021) R: a language and environment for statistical computing. R Foundation for Statistical Computing, Vienna, Austria. http://www.R- project.org.

Rezaee S, Kia-Daliri H, Sharifi K, Ahangaran Y, Hajmansoor S (2013) Boxwood blight caused by *Cylindrocladium buxicola* in Tonekabon forest. Applied Entomology and Phytopathology 80: 197–198.

Ricciardi A, Blackburn TM, Carlton JT, Dick JTA, Hulme PE, Iacarella JC, Jeschke JM, Liebhold AM, Lockwood JL, MacIsaac HJ, Pyšek P, Richardson DM, Ruiz GM, Simberloff D, Sutherland WJ, Wardle DA, Aldridge DC (2017) Invasion science: a horizon scan of emerging challenges and opportunities. Trends in Ecology and Evolution 32: 464–474. https://doi.org/10.1016/j.tree.2017.03.007

Richardson PA, Daughtrey M, Hong C (2020) Indications of susceptibility to *Calonectria pseudonaviculata* in some common groundcovers and boxwood companion plants. Plant Disease 104: 1127–1132. https://doi.org/10.1094/PDIS-08-19-1582-RE

1169 Ryan C, Williams-Woodward J, Zhang DL (2018) Susceptibility of *Sarcococca* taxa to boxwood
1170 blight by *Calonectria pseudonaviculata*. In: Proceedings of southern nursery association
1171 research conference, vol. 62. , 64–67.
1172 Safránková I, Kmoch M, Holková L (2012) First report of *Cylindrocladium buxicola* on box in
1173 Czech Republic. New Disease Reports 25: 5. https://doi.org/10.2307/3761865
1174 Salvesen PH, Kanz B (2009) Boxwood cultivars in old gardens in Norway. In: Morel J-P,
1175 Mercuri AM (Eds), Plants and Culture: Seeds of the Cultural Heritage of Europe. Edipuglia,
1176 Puglia, Italy, 247–262. Available from: http://www.plants-culture.unimore.it/book.htm.
1177 Santini A, Ghelardini L, De Pace C, Desprez-Loustau ML, Capretti P, Chandelier A, Cech T,
1178 Chira D, Diamandis S, Gaitniekis T, Hantula J, Holdenrieder O, Jankovsky L, Jung T, Jurc
1179 D, Kirisits T, Kunca A, Lygis V, Malecka M, Marcais B, Schmitz S, Schumacher J,
1180 Solheim H, Solla A, Szabò I, Tsopelas P, Vannini A, Vettraino AM, Webber J, Woodward
1181 S, Stenlid J (2013) Biogeographical patterns and determinants of invasion by forest
1182 pathogens in Europe. New Phytologist 197: 238–250. https://doi.org/10.1111/j.1469-
1183 8137.2012.04364.x
1184 Saracchi M, Rocchi F, Pizzatti C, Cortesi P (2008) Box blight, a new disease of *Buxus* in Italy
1185 caused by *Cylindrocladium buxicola*. Journal of Plant Pathology 90: 581–584.
1186 https://doi.org/10.4454/jpp.v90i3.703
1187 Saurat C, Fourrier C, Ioos R (2012) First report of blight disease on *Buxus* caused by
1188 *Cylindrocladium buxicola* in France. Plant Disease 96: 1069–1069.
1189 https://doi.org/https://doi.org/10.1094/PDIS-03-12-0242-PDN
1190 Schatz GE, Lowry PPI (2002) A synoptic revision of the genus *Buxus* L. (Buxaceae) in
1191 Madagascar and the Comoro Islands. Adansonia 24: 179–196.
1192 Senay SD, Worner SP, Ikeda T (2013) Novel three-step pseudo-absence selection technique for
1193 improved species distribution modelling. PLoS ONE 8: e71218.
1194 https://doi.org/10.1371/journal.pone.0071218
1195 Shabani F, Kumar L, Ahmadi M (2016) A comparison of absolute performance of different
1196 correlative and mechanistic species distribution models in an independent area. Ecology and
1197 Evolution 6: 5973–5986. https://doi.org/10.1002/ece3.2332
1198 Shishkoff N, Camp MJ (2016) The effect of different temperatures and moisture levels on
1199 survival of *Calonectria pseudonaviculata* in boxwood leaves and twigs and as

microsclerotia produced in culture. Plant Disease 100: 2018–2024. https://doi.org/10.1094/PDIS-09-15-1098-RE

Shishkoff N, Daughtrey M, Aker S, Olsen RT, Disease UF, Science W, Daughtrey M, Island L (2015) Evaluating boxwood susceptibility to *Calonectria pseudonaviculata* using cuttings from the national boxwood collection. Plant Health Progress 16: 11–15. https://doi.org/10.1094/php-rs-14-0033

Şimşek SA, Katırcıoğlu YZ, Çakar D, Rigling D, Maden S (2019) Impact of fungal diseases on common box (*Buxus sempervirens* L.) vegetation in Turkey. European Journal of Plant Pathology 153: 1203–1220. https://doi.org/10.1007/s10658-018-01636-4

Van der Straten MJ, Muus TST (2010) The box tree pyralid, *Glyphodes perspectalis* (Lepidoptera: Crambidae), an invasive alien moth ruining box trees. Proceedings of the Netherlands Entomological Society Meeting 21: 107–111. Available from: http://www.nev.nl/pages/publicaties/proceedings/nummers/21/1-136.pdf#page=107.

Sutherst RW (2014) Pest species distribution modelling: origins and lessons from history. Biological Invasions 16: 239–256. https://doi.org/10.1007/s10530-013-0523-y

Sutherst RW, Maywald GF (1985) A computerised system for matching climates in ecology. Agriculture, Ecosystems and Environment 13: 281–299. https://doi.org/10.1016/0167-8809(85)90016-7

Taylor S, Kumar L (2012) Sensitivity analysis of CLIMEX parameters in modelling potential distribution of *Lantana camara* L. PLoS ONE 7: e40969. https://doi.org/10.1371/journal.pone.0040969

Thakur MP, van der Putten WH, Cobben MMP, van Kleunen M, Geisen S (2019) Microbial invasions in terrestrial ecosystems. Nature Reviews Microbiology 17: 621–631. https://doi.org/10.1038/s41579-019-0236-z

Thuiller W (2004) Patterns and uncertainties of species' range shifts under climate change. Global Change Biology 10: 2020–2027. https://doi.org/10.1111/j.1365-2486.2004.00859.x

United States Department of Agriculture (1976) Growing boxwoods. U.S. Department of Agriculture, Washington, D.C.

USDA National Agricultural Statistics Service (2020) Census of Horticultural Specialties. Available at: https://www.nass.usda.gov/Publications/AgCensus/2017/Online_Resources/Census_of_Hor

ticulture_Specialties/.

USGCRP (2018) Impacts, Risks, and Adaptation in the United States: Fourth National Climate Assessment, Volume II. Reidmiller DR, Avery CW, Easterling DR, Kunkel KE, Lewis KLM, Maycock TK, Stewar BC (Eds). U.S. Global Change Research Program, Washington, DC, USA, 1515 pp. https://doi.org/10.7930/NCA4.2018

Vale CG, Tarroso P, Brito JC (2014) Predicting species distribution at range margins: testing the effects of study area extent, resolution and threshold selection in the Sahara-Sahel transition zone. Diversity and Distributions 20: 20–33. https://doi.org/10.1111/ddi.12115

Veloz SD (2009) Spatially autocorrelated sampling falsely inflates measures of accuracy for presence-only niche models. Journal of Biogeography 36: 2290–2299. https://doi.org/10.1111/j.1365-2699.2009.02174.x

Watling JI, Brandt LA, Bucklin DN, Fujisaki I, Mazzotti FJ, Romañach SS, Speroterra C (2015) Performance metrics and variance partitioning reveal sources of uncertainty in species distribution models. Ecological Modelling 309–310: 48–59. https://doi.org/10.1016/j.ecolmodel.2015.03.017

Yang X, Hong C (2018) Microsclerotial enumeration, size, and survival of *Calonectria pseudonaviculata*. Plant Disease 102: 983–990. https://doi.org/10.1094/PDIS-08-17-1249-RE

Zurell D, Elith J, Schröder B (2012) Predicting to new environments: Tools for visualizing model behaviour and impacts on mapped distributions. Diversity and Distributions 18: 628–634. https://doi.org/10.1111/j.1472-4642.2012.00887.x

Tables and Figures

Table 1. CLIMEX parameter values for *Calonectria pseudonaviculata*.

Table 2. Summary of the principal component analysis of 27 bioclimatic variables used for correlative models. Principal component (PC) axes were selected until the cumulative explanation proportion reached 95% or more of the total variation of the original matrix. Loadings of PCs for each variable are presented, as well as PC's eigenvalues, the proportion of explained variance of each PC, and accumulated proportion of explained variance. The largest loadings (positive or negative) for each component (>0.30) are indicated with bold font.

Table 3. Mean values of evaluation statistics for individual correlative models and the ensemble model.

Table 4. The percent contribution of each principal component (PC) variable to correlative models produced by six algorithms. The climatic relevance of each variable [based on which bioclimatic variables had the largest loadings (positive or negative, Table 2)] and the average and range of contributions across all algorithms is indicated.

Figure 1. Maps of climatic suitability and potential distribution for *Calonectria pseudonaviculata* in Europe and western Asia. Climatic suitability is estimated as the ecoclimatic index in the CLIMEX model **A** with and **B** without irrigation, and as **C** the probability of occurrence in the ensemble correlative model. Areas of overlap in the potential distribution (purple shading) according to both CLIMEX models (ecoclimatic index = 10–100) and the ensemble correlative model (presence predictions) are shown in comparison to areas that were included in the potential distribution by only one model [red shading = CLIMEX model (no irrigation); orange shading = CLIMEX model (including irrigation); blue shading = ensemble correlative model]. Black circles represent the approximate locations of occurrence records.

Figure 2. Population growth and climate stress accumulation for *Calonectria pseudonaviculata* in Europe and western Asia. Population growth in CLIMEX is measured as the **A** annual growth

index (annual growth index, range = 0–100). Climate stress indices (range = 0–999) include **B** cold stress, **C** heat stress, and **D** dry stress. Results are for the CLIMEX model which did not include irrigation.

Figure 3. Maps of climatic suitability and the potential distribution for *Calonectria pseudonaviculata* in North America. Climatic suitability is estimated as the ecoclimatic index in the CLIMEX model **A** with and **B** without irrigation, and as **C** the probability of occurrence in the ensemble correlative model. Areas of overlap in the potential distribution (purple shading) according to both CLIMEX models (ecoclimatic index = 10–100) and the ensemble correlative model (presence predictions) are shown in comparison to areas that were included in the potential distribution by only one model [red shading = CLIMEX model (no irrigation); orange shading = CLIMEX model (including irrigation); blue shading = ensemble correlative model]. Black circles represent the approximate locations of occurrence records.

Figure 4. Population growth and climate stress accumulation for *Calonectria pseudonaviculata* in North America. Population growth in CLIMEX is measured as the **A** annual growth index (annual growth index, range = 0–100). Climate stress indices (range = 0–999) include **B** cold stress, **C** heat stress, and **D** dry stress.

Figure 5. Climatic suitability for *Calonectria pseudonaviculata* globally. Climatic suitability is estimated as **A** the ecoclimatic index in the CLIMEX model (includes irrigation), and as **B** the probability of occurrence in the ensemble correlative model. Areas where the ecoclimatic index is zero and the probability of occurrence is less than 0.1 are shown in gray.

Figure 6. Map of the global potential distribution for *Calonectria pseudonaviculata*. Areas of overlap in the potential distribution (purple shading) according to both CLIMEX models (ecoclimatic index = 10–100) and the ensemble correlative model (presence predictions) are shown in comparison to areas that were included in the potential distribution by only one model (red shading = CLIMEX model; orange shading = CLIMEX model that included irrigation; blue shading = ensemble correlative model).

Figure 7. Mobility-oriented parity (MOP) assessment outputs for projections of the ensemble correlative model for *Calonectria pseudonaviculata*. Areas with MOP metric values close to 1 have highly comparable climatic conditions to the those in the model calibration area. Areas with values approaching 0 indicate higher extrapolation because one or more climatic variables have values outside the range of variable(s) in the calibration area.

Figure 8. Climate comparisons for sites which are expected to differ in favorability for boxwood blight infections. Line plots depict monthly temperature (solid lines) and precipitation (dashed lines) across eight sites in Europe (orange lines) and the United States (blue lines). Sites with a Mediterranean climate (e.g., Cannes, France; Naples, Italy; Seattle, Washington; and Portland, Oregon) are less conducive for infections than sites which have higher humidity, few gaps in precipitation, and ideal temperatures for growth throughout the year, such as those in temperate/coastal climates in western Europe (e.g., Brussels, Belgium and Bordeaux, France) and warm and humid climates in the mid-Atlantic and southeastern regions of the United States (e.g., Virginia Beach, Virginia and Atlanta, Georgia). Data source: 1981-2010 climate normals, World Meteorological Organization (https://climatedata-catalogue.wmo.int; accessed 24 Sep 2021).

1333 **Table 1.** CLIMEX parameter values for *Calonectria pseudonaviculata*.

1334

Parameter	Description	Value
Parameter		
SM0	Limiting low moisture	0.2
SM1	Lower optimal moisture	0.7
SM2	Upper optimal moisture	1.7
SM3	Limiting high moisture	3.0
Temperature		
DV0	Limiting low temperature (°C)	8
DV1	Lower optimal temperature (°C)	21
DV2	Upper optimal temperature (°C)	25
DV3	Limiting high temperature (°C)	29
Cold stress		
TTCS	Cold stress temperature threshold (°C)	–10
TCCS	Cold stress temperature rate (week^{-1})	–0.005
Heat stress		
TTHS	Heat stress temperature threshold (°C)	32
THHS	Heat stress temperature rate (week^{-1})	0.01
Dry stress		
SMDS	Dry stress threshold	0.2
HDS	Dry stress rate (week^{-1})	–0.001
Wet stress		
SMWS	Wet stress threshold	3.0
HWS	Wet stress rate (week^{-1})	0.005

1335 **Table 2.** Summary of the principal component analysis of 27 bioclimatic variables used for
1336 correlative models. Principal component (PC) axes were selected until the cumulative
1337 explanation proportion reached 95% or more of the total variation of the original matrix.
1338 Loadings of PCs for each variable are presented, as well as PC's eigenvalues, the proportion of
1339 explained variance of each PC, and accumulated proportion of explained variance. The largest
1340 loadings (positive or negative) for each component (>0.30) are indicated with bold font.
1341

Variables and proportion of variance	PC1	PC2	PC3	PC4	PC5	PC6
Variable						
Annual mean temperature (bio1)	0.033	0.212	0.298	–0.001	–0.001	–0.014
Mean diurnal temperature range (bio2)	0.083	–0.164	0.261	–0.226	**–0.369**	–0.199
Isothermality (bio3)	0.012	0.235	0.082	–0.192	–0.271	–0.066
Temperature seasonality (bio4)	0.06	**–0.484**	0.06	0.006	0.039	0.023
Max temperature of warmest week (bio5)	0.12	–0.013	**0.404**	–0.023	–0.023	–0.068
Min temperature of coldest week (bio6)	0.023	**0.365**	0.151	0.027	0.035	–0.003
Temperature annual range (bio7)	0.095	**–0.562**	0.208	–0.065	–0.077	–0.069
Mean temperature of wettest quarter (bio8)	–0.317	–0.024	**0.566**	0.07	0.118	**0.361**
Mean temperature of driest quarter (bio9)	0.204	0.246	0.098	–0.029	–0.04	–0.184
Mean temperature of warmest quarter (bio10)	0.082	0.051	**0.4**	0.006	0.019	–0.017
Mean temperature of coldest quarter (bio11)	0.013	**0.321**	0.187	–0.004	–0.019	–0.017
Annual precipitation (bio12)	–0.075	–0.002	0.019	–0.3	0.054	–0.179
Precipitation of wettest week (bio13)	–0.059	–0.027	0.016	**–0.484**	0.073	0.066
Precipitation of driest week (bio14)	–0.142	0.034	–0.009	–0.054	–0.041	**–0.415**
Precipitation seasonality (bio15)	0.001	0.095	–0.169	**–0.389**	–0.258	**0.574**
Precipitation of wettest quarter (bio16)	–0.056	–0.025	0.012	**–0.464**	0.077	0.035
Precipitation of driest quarter (bio17)	–0.132	0.028	0.003	–0.075	–0.028	**–0.405**
Precipitation of warmest quarter (bio18)	**–0.386**	–0.054	0.141	–0.157	–0.004	–0.01
Precipitation of coldest quarter (bio19)	0.174	0.033	–0.08	**–0.373**	0.091	–0.216
Annual mean moisture index (bio28)	–0.138	0.012	–0.011	–0.041	0.27	–0.041
Highest weekly moisture index (bio29)	0.032	–0.005	0.007	–0.112	**0.427**	0.041
Lowest weekly moisture index (bio30)	**–0.317**	0.032	–0.075	0.001	0.036	–0.082
Moisture index seasonality (bio31)	**0.497**	0.052	0.013	–0.101	0.195	0.09
Mean moisture index of wettest quarter (bio32)	0.026	–0.005	0.008	–0.093	**0.426**	0.024
Mean moisture index of driest quarter (bio33)	–0.31	0.03	–0.061	–0.004	0.055	–0.08
Mean moisture index of warmest quarter (bio34)	**–0.345**	0.036	–0.093	–0.054	0.02	0.003
Mean moisture index of coldest quarter (bio35)	0.051	–0.003	0.072	–0.036	**0.44**	–0.077
Proportion of variance						
Proportion explained by each PC (%)	52.2	27.3	6.4	4.1	3.2	2.6
Accumulated proportion explained by the PCs (%)	52.2	79.5	85.9	90	93.2	95.8

1342 **Table 3**. Mean values of evaluation statistics for individual correlative models and the ensemble model.

1343

Algorithm	AUC	Kappa	TSS	Jaccard	Sørensen	F_{pb}
Boosted regression tree	0.998	0.974	0.974	0.975	0.987	1.949
Generalized additive models	0.996	0.986	0.986	0.986	0.993	1.972
Bayesian Gaussian process	0.999	0.982	0.982	0.982	0.991	1.965
Maxent	0.998	0.974	0.974	0.975	0.987	1.949
Random forests	0.998	0.978	0.978	0.978	0.989	1.956
Support vector machine	1	0.992	0.992	0.992	0.996	1.984
Ensemble	1	0.996	0.996	0.996	0.998	1.992

1344

1345 AUC, Area Under the ROC Curve; TSS, True Skill Statistics; F_{pb}, F-measure on presence-background

1346

1347 **Table 4.** The percent contribution of each principal component (PC) variable to correlative models produced by six algorithms. The
1348 climatic relevance of each variable [based on which bioclimatic variables had the largest loadings (positive or negative, Table 2)] and
1349 the average and range of contributions across all algorithms is indicated.
1350

Variable	Climatic relevance	BRT	GAM	GAU	MXS	RDF	SVM	Average (%)
PC1	Warm season precipitation and soil moisture, soil moisture seasonality	29.4	23.9	21.4	22.7	26.9	21.4	24.3 (21.4–29.4)
PC2	Cold season temperatures, temperature seasonality	60	23.9	47.3	45.2	61.6	44.2	47 (23.9–61.6)
PC3	Warm and wet season temperatures	0.3	22.2	9.2	8.9	1.1	9.4	8.5 (0.3–22.2)
PC4	Wet season precipitation	0.7	10	5.3	6.3	0.2	6.4	4.8 (0.2–10)
PC5	Diurnal temperature range, wet and cold season soil moisture	9.3	10	9	9.5	10	10.9	9.8 (9–10.9)
PC6	Dry season precipitation, precipitation seasonality	0.4	10	7.8	7.4	0.3	7.7	5.6 (0.3–10)

1351
1352 BRT, boosted regression tree; GAM, generalized additive models; GAU, Gaussian process; MXS, Maxent “simple”; RDF, random
1353 forests; SVM, support vector machine.

Figure 1. Maps of climatic suitability and potential distribution for *Calonectria pseudonaviculata* in Europe and western Asia. Climatic suitability is estimated as the ecoclimatic index in the CLIMEX model **A** with and **B** without irrigation, and as **C** the probability of occurrence in the ensemble correlative model. Areas of overlap in the potential distribution (purple shading) according to both CLIMEX models (ecoclimatic index = 10–100) and the ensemble correlative model (presence predictions) are shown in comparison to areas that were included in the potential distribution by only one model [red shading = CLIMEX model (no irrigation); orange shading = CLIMEX model (including irrigation); blue shading = ensemble correlative model]. Black circles represent the approximate locations of occurrence records.

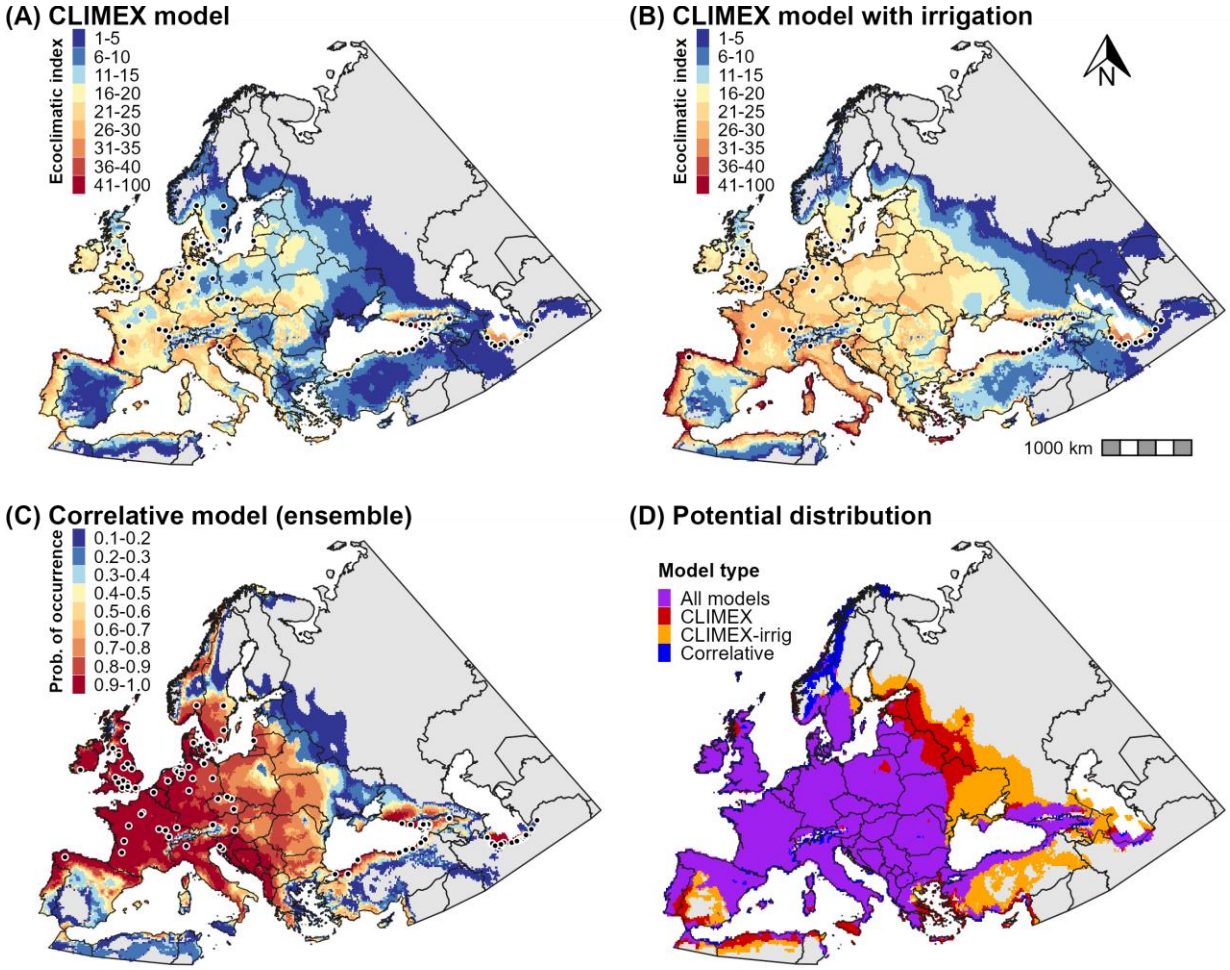

Figure 2. Population growth and climate stress accumulation for *Calonectria pseudonaviculata* in Europe and western Asia. Population growth in CLIMEX is measured as the **A** annual growth index (annual growth index, range = 0–100). Climate stress indices (range = 0–999) include **B** cold stress, **C** heat stress, and **D** dry stress. Results are for the CLIMEX model which did not include irrigation.

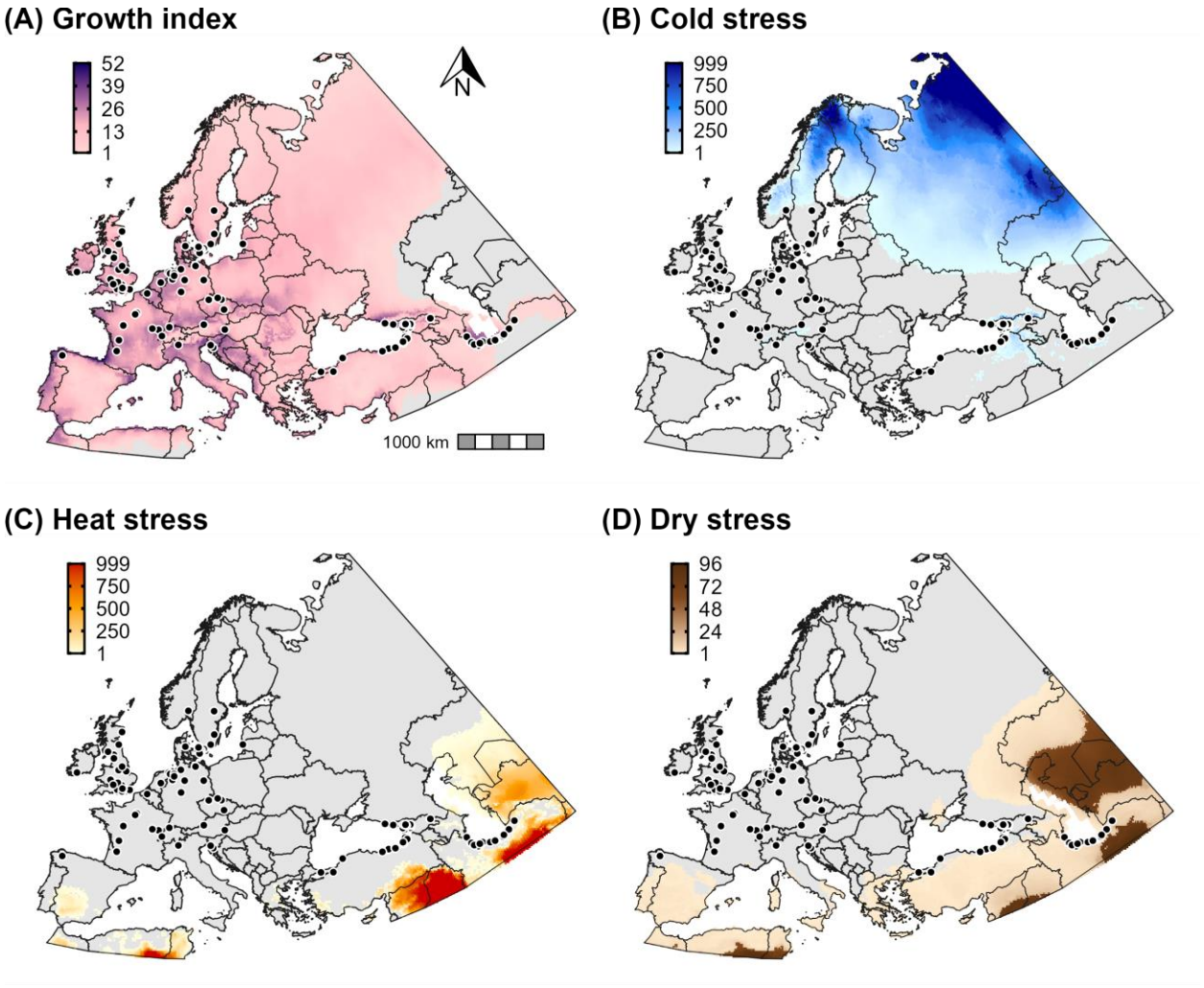

Figure 3. Maps of climatic suitability and the potential distribution for *Calonectria pseudonaviculata* in North America. Climatic suitability is estimated as the ecoclimatic index in the CLIMEX model **A** with and **B** without irrigation, and as **C** the probability of occurrence in the ensemble correlative model. Areas of overlap in the potential distribution (purple shading) according to both CLIMEX models (ecoclimatic index = 10–100) and the ensemble correlative model (presence predictions) are shown in comparison to areas that were included in the potential distribution by only one model [red shading = CLIMEX model (no irrigation); orange shading = CLIMEX model (including irrigation); blue shading = ensemble correlative model]. Black circles represent the approximate locations of occurrence records.

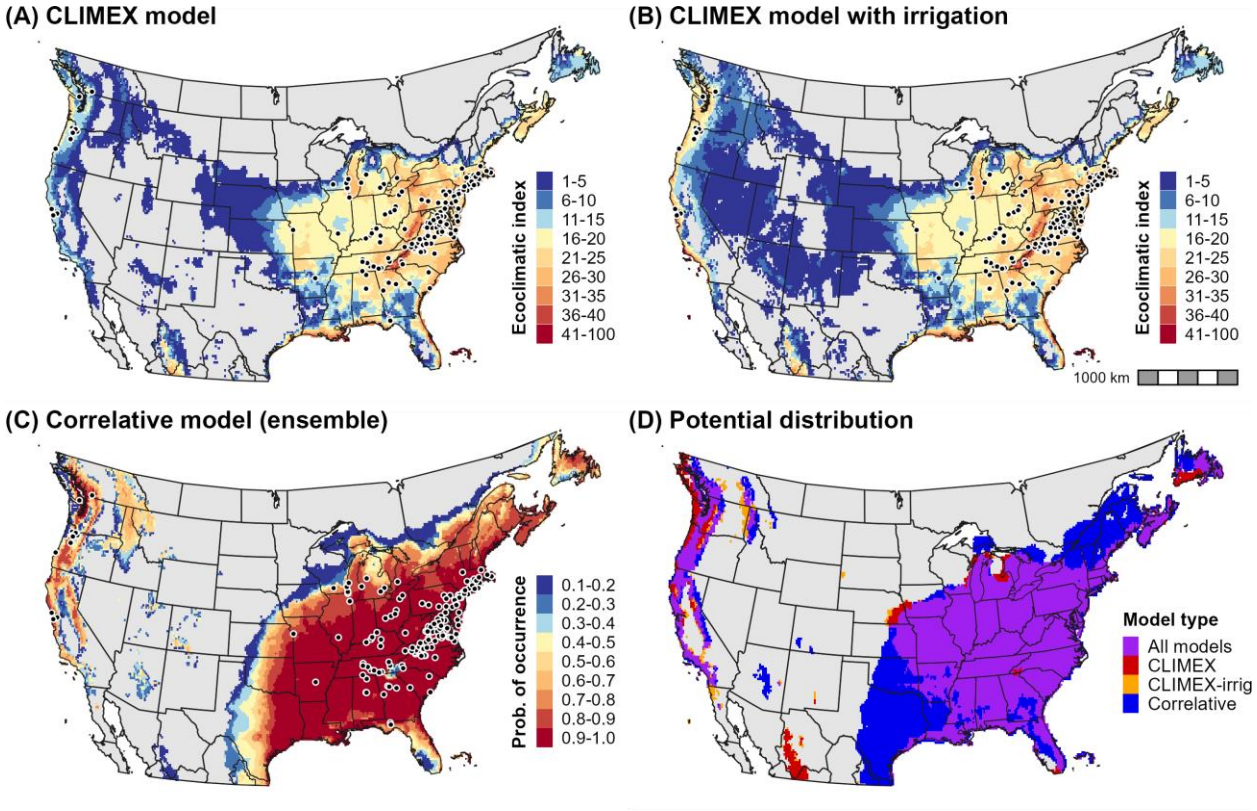

Figure 4. Population growth and climate stress accumulation for *Calonectria pseudonaviculata* in North America. Population growth in CLIMEX is measured as the **A** annual growth index (annual growth index, range = 0–100). Climate stress indices (range = 0–999) include **B** cold stress, **C** heat stress, and **D** dry stress.

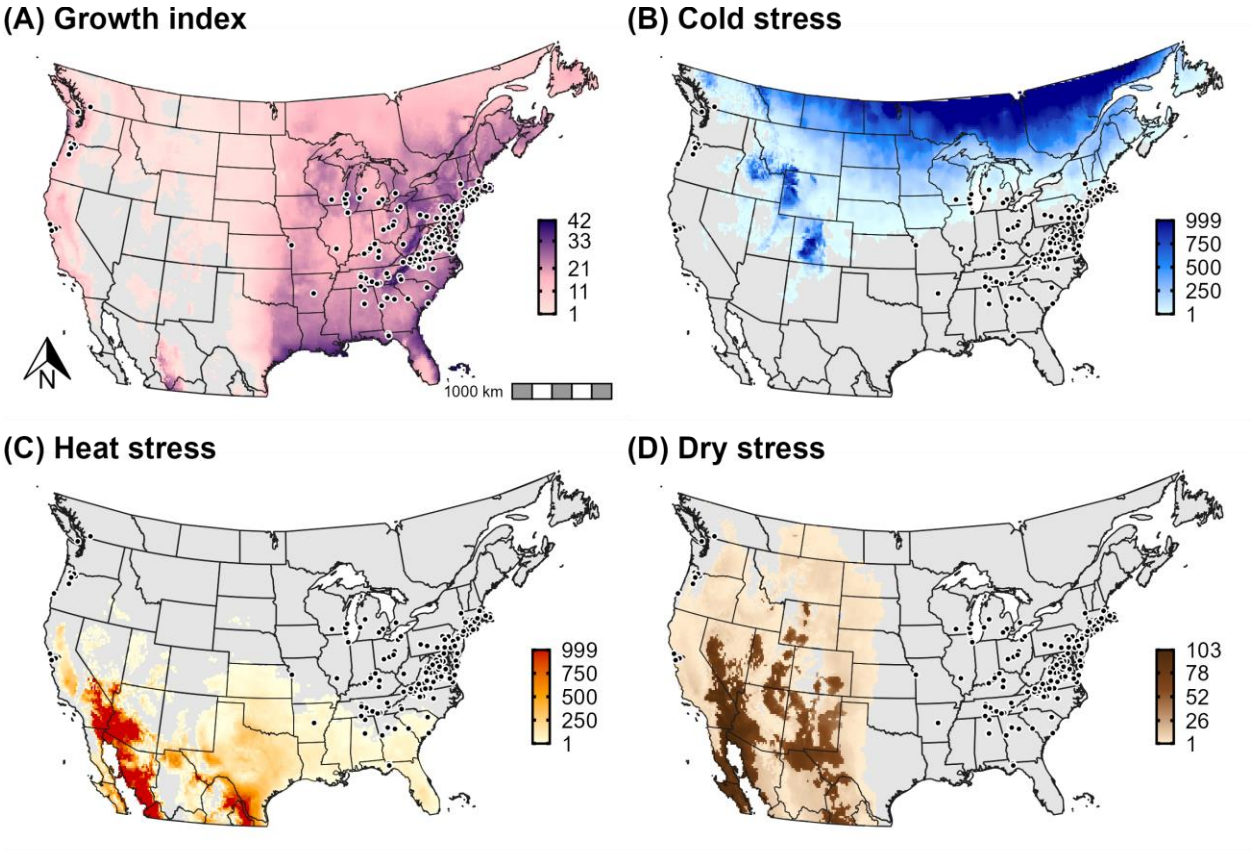

Figure 5. Climatic suitability for *Calonectria pseudonaviculata* globally. Climatic suitability is estimated as **A** the ecoclimatic index in the CLIMEX model (includes irrigation), and as **B** the probability of occurrence in the ensemble correlative model. Areas where the ecoclimatic index is zero and the probability of occurrence is less than 0.1 are shown in gray.

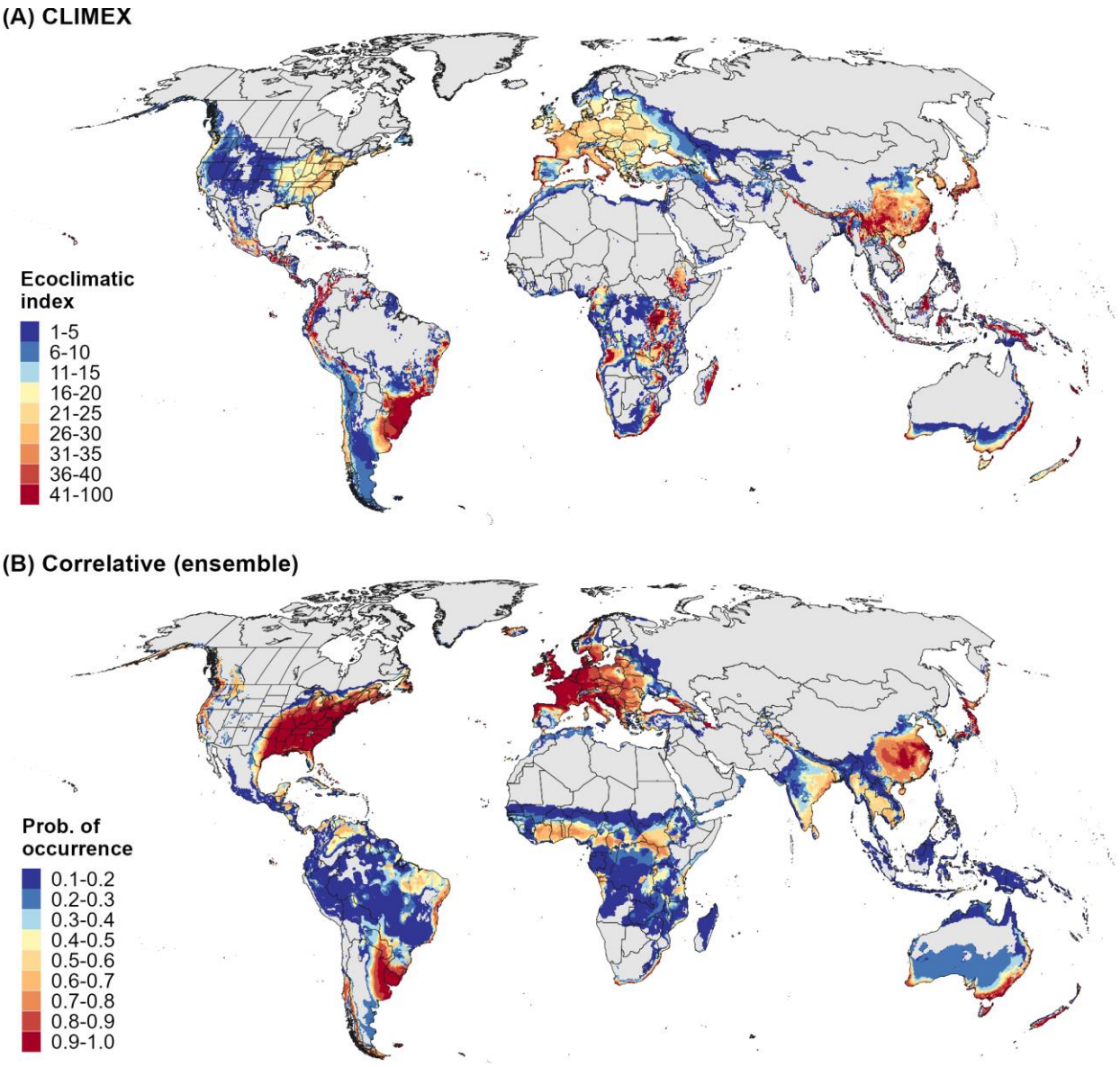

Figure 6. Map of the global potential distribution for *Calonectria pseudonaviculata*. Areas of overlap in the potential distribution (purple shading) according to both CLIMEX models (ecoclimatic index = 10–100) and the ensemble correlative model (presence predictions) are shown in comparison to areas that were included in the potential distribution by only one model (red shading = CLIMEX model; orange shading = CLIMEX model that included irrigation; blue shading = ensemble correlative model).

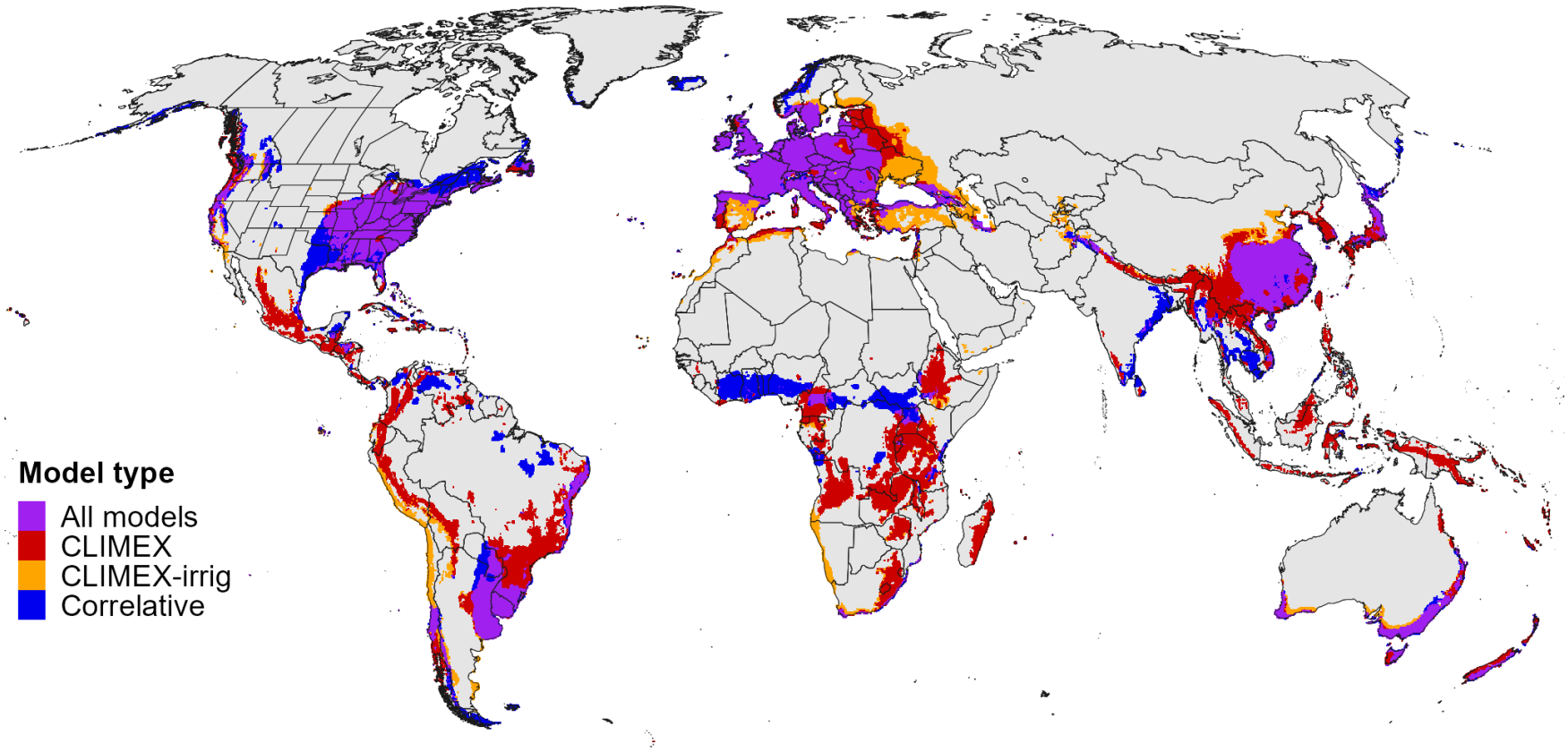

Figure 7. Mobility-oriented parity (MOP) assessment outputs for projections of the ensemble correlative model for *Calonectria pseudonaviculata*. Areas with MOP metric values close to 1 have highly comparable climatic conditions to the those in the model calibration area. Areas with values approaching 0 indicate higher extrapolation because one or more climatic variables have values outside the range of variable(s) in the calibration area.

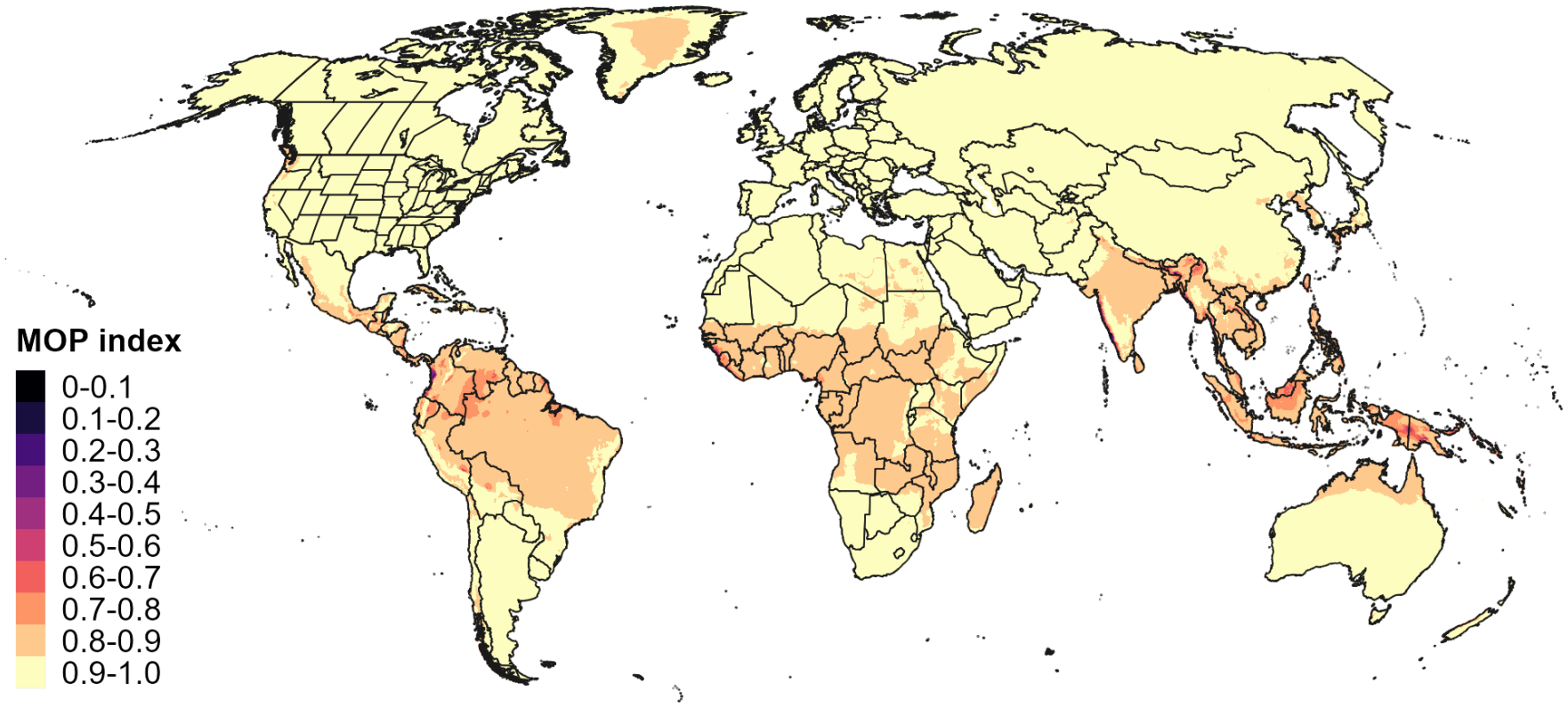

Figure 8. Climate comparisons for sites which are expected to differ in favorability for boxwood blight infections. Line plots depict monthly temperature (solid lines) and precipitation (dashed lines) across eight sites in Europe (orange lines) and the United States (blue lines). Sites with a Mediterranean climate (e.g., Cannes, France; Naples, Italy; Seattle, Washington; and Portland, Oregon) are less conducive for infections than sites which have higher humidity, few gaps in precipitation, and ideal temperatures for growth throughout the year, such as those in temperate/coastal climates in western Europe (e.g., Brussels, Belgium and Bordeaux, France) and warm and humid climates in the mid-Atlantic and southeastern regions of the United States (e.g., Virginia Beach, Virginia and Atlanta, Georgia). Data source: 1981-2010 climate normals, World Meteorological Organization (https://climatedata-catalogue.wmo.int; accessed 24 Sep 2021).